

1 **Drainage reorganization and divide migration induced by the excavation of the Ebro**  
2 **basin (NE Spain)**

3

4 Arnaud Vacherat <sup>1</sup>, Stéphane Bonnet <sup>1</sup>, Frédéric Mouthereau <sup>1</sup>

5

6 <sup>1</sup>Géosciences Environnement Toulouse (GET), Université de Toulouse, CNRS, IRD, UPS,  
7 (Toulouse), France

8

9 *Correspondance to:* Stéphane Bonnet (stephane.bonnet@get.omp.eu)

10

11 **Abstract**

12

13 Intracontinental endorheic basins are key elements of source-to-sink systems as they preserve  
14 sediments eroded from the surrounding catchments. Drainage reorganization in such a basin in  
15 response to changing boundary conditions has strong implications on the sediment routing  
16 system and on landscape evolution. The Ebro and Duero basins represent two foreland basins,  
17 which developed in response to the growth of surrounding compressional orogens, the Pyrenees  
18 and the Cantabrian mountains to the north, the Iberian Ranges to the south, and the Catalan  
19 Coastal Range to the east. They were once connected as endorheic basins in the early Oligocene.  
20 By the end of the Miocene, new post-orogenic conditions led to the current setting in which the  
21 Ebro and Duero basins are flowing in opposite directions, towards the Mediterranean Sea and  
22 the Atlantic Ocean. Although these two hydrographic basins recorded a similar history, they are  
23 characterized by very different morphologic features. The Ebro basin is highly excavated,  
24 whereas relicts of the endorheic stage are very well preserved in the Duero basin. The  
25 contrasting morphological preservation of the endorheic stage represents an ideal natural  
26 laboratory to study the drivers (internal / external) of post-orogenic drainage divide mobility,  
27 drainage network and landscape evolution. To that aim, we use field and map observations and  
28 we apply the  $\chi$ -analysis of river profiles along the divide between the Ebro and Duero drainage  
29 basins. We show here that the contrasting excavation of the Ebro and Duero basins drives a  
30 reorganization of their drainage network through a series of captures, which resulted in the  
31 southwestward migration of their main drainage divide. Fluvial captures have strong impact on  
32 drainage areas, fluxes, and so on their respective incision capacity. We conclude that drainage  
33 reorganization driven by the capture of the Duero rivers by the Ebro drainage system explains

34 the first-order preservation of endorheic stage remnants in the Duero basin, due to drainage area  
35 loss, independently from tectonics and climate.

36

## 37 **1. Introduction**

38

39 Landscapes subjected to contrasted erosion rates between adjacent drainage basins show a  
40 migration of their drainage divide toward the area of lower erosion rates (Bonnet, 2009; Willett  
41 et al., 2014). This is the case for mountain ranges characterized by gradients in precipitation  
42 rates due to orography, once landscapes are in a transient state and are not adjusted to  
43 precipitation differences (Bonnet, 2009). It also occurs when drainage reorganized in response  
44 to capture (Yanites et al., 2013; Willett et al., 2014). River capture actually drives a discrete  
45 drop in the location of drainage divide (Prince et al. 2011) but also produces a wave of erosion  
46 in the captured reach (Yanites et al., 2013) that may impact divide position. Historically,  
47 migration of divides has been inferred by changes in the provenance of sediments stored in  
48 sedimentary basins (*e.g.* Kuhlemann et al., 2001). It is however a process that is generally very  
49 difficult to document in erosional landscapes. Recent developments have provided models and  
50 analytical approaches to identify divide migration in the landscape (Bonnet, 2009; Castelltort  
51 et al., 2012; Willett et al., 2014; Whipple et al., 2017). Among them the recently-developed  $\chi$ -  
52 method for analyzing longitudinal profiles of rivers (Perron and Royden, 2012) is based on the  
53 recognition of disequilibrium along river profiles, disequilibrium being defined by the departure  
54 from an ideal equilibrium shape. The application of this method to both natural and numerically-  
55 simulated landscapes, has allowed to demonstrate contrasts in the equilibrium state of rivers  
56 across divide and then to infer their migration (Willett et al., 2014). The applicability of this  
57 method is however limited to settings where the response time of rivers is larger compared to  
58 the rate of divide migration, so they can actually show disequilibrium in their longitudinal  
59 profiles (Whipple et al., 2017).

60

61 The Ebro and Duero drainage basins in the Northern Iberian Peninsula show geological and  
62 geomorphological evidence of very contrasted erosional histories during the Neogene. They  
63 initially recorded a long endorheic stage from the Early Oligocene to the Late Miocene. Since  
64 then, both basins opened toward the Atlantic Ocean (Duero) or the Mediterranean Sea (Ebro).  
65 The Ebro basin's opening is reflected in the landscape by evidence of river incision (Garcia-  
66 Castellanos et al., 2003), whereas the Duero Basin does not show significant incision in its  
67 upstream part as a large relict of its endorheic morphology is preserved (Antón et al., 2012).

68 The Duero river long profile actually shows a pronounced knickpoint (knickzone) defining an  
69 upstream domain of high mean elevation (~800 m) and low relief where the sediments deposited  
70 during the endorheic stage are relatively well preserved. Then, these two adjacent basins are  
71 characterized by contrasting preservation of their endorheic stages and represent an ideal natural  
72 laboratory to evaluate the mechanisms that caused differential post-orogenic incision at the  
73 origin of divide migration. Following a presentation of the geological context, we first compile  
74 evidence of fluvial captures along the Ebro-Duero divide, based on previous studies and our  
75 own investigations, and we map the location of knickpoints and relict portions of the drainage  
76 network. We use all these observations to reconstruct a paleo-divide position and to estimate  
77 the impact of divide migration in terms of drainage area and stream power. We complement  
78 this dataset by providing a map of  $\chi$  across divide (Willett et al., 2014) to highlight potential  
79 disequilibrium state between rivers of the Ebro and Duero catchments.

80

## 81 **2. Geological setting**

82

### 83 2.1 The Ebro and Duero basins

84

85 The Ebro and Duero basins represent two hydrographic basins located in the northern part of  
86 the Iberian Peninsula (Fig. 1). The bedrock of the Ebro and Duero drainage basins mainly  
87 consists of Cenozoic deposits, and Mesozoic and Paleozoic rocks in their headwaters (Fig. 2).  
88 They formed once a unique foreland basin during the Cenozoic controlled by the flexural  
89 loading by the surrounding mountain belts: the Pyrenees and the Cantabrian mountains to the  
90 north (Pulgar et al., 1999), the Iberian and Central Ranges to the south (Guimerà et al., 2004;  
91 De Vicente et al., 2007), and the Catalan Coastal Range (CCR) to the east (López-Blanco et al.,  
92 2000 ; Salas et al., 2001), during collision between Iberia and Europe since the Late Cretaceous.

93

94 From the Late Cretaceous, the Ebro and Duero basins were essentially filled by clastic deposits,  
95 and opened toward the Atlantic Ocean in the Bay of Biscay (Alonso-Zarza et al., 2002). During  
96 the Late Eocene – Early Oligocene, the uplift in the Western Pyrenees (Puigdefàbregas et al.,  
97 1992) led to the closure of the Ebro and Duero basins as attested by the Ebro basin  
98 continentalization dated at ~36 Ma (Costa et al., 2010). The center of these two basins became  
99 long-lived lakes filled with lacustrine, sandy, and evaporitic deposits from the Oligocene to the  
100 Miocene (Riba et al., 1983; Alonso-Zarza et al., 2002; Pérez-Rivarés et al., 2002, 2004; Garcia-  
101 Castellanos et al, 2003; Garcia-Castellanos, 2006; Larrasoaña et al., 2006; Vázquez-Urbez et

102 al., 2013). The opening of the Ebro basin through the Catalan Coastal Range toward the  
103 Mediterranean Sea occurred during the Late Miocene, leading to kilometer-scale excavation  
104 throughout the basin (Fillon and Van der Beek, 2012; Fillon et al., 2013; Garcia-Castellanos  
105 and Larrasoña, 2015). The exact timing and processes driving the opening, as well as the  
106 role of the Messinian Salinity Crisis, have long been debated (Coney et al., 1996 (post-  
107 Messinian); Garcia-Castellanos et al., 2003 (13-8.5 Ma); Babault et al., 2006 (post-Messinian);  
108 Urgeles et al., 2010; Cameselle et al. (2014) (Serravallian-Tortonian); Garcia-Castellanos and  
109 Larrasoña, 2015 (12-7.5 Ma)). In contrast with the Ebro basin, incision in the upper Duero  
110 basin appears much less significant. The Duero basin is characterized by a low relief topography  
111 (Fig. 1) in its upstream part, at 700-800 m above sea level to the west, and at 1000-1100 m a.s.l.  
112 to the north, northeast, and to the east in the Almazan subbasin, close to the divide with the  
113 Ebro basin. The connection of the Duero River with the Atlantic Ocean occurred from the Late  
114 Miocene-Early Pliocene to the Late Pliocene-Early Pleistocene (Martín-Serrano, 1991). The  
115 current Ebro and Duero drainage networks are separated by a divide running from the  
116 Cantabrian belt to the NW, toward the SE in the Iberian Range (Figs. 1, 2, 3). In the following,  
117 we review the geological evolution of the different domains that constitute this drainage divide  
118 between the Ebro and Duero drainage basins.

119

## 120 2.2 The Iberian Range

121

122 The Iberian Range (Figs. 2, 4) is a double vergent fold-and-thrust belt resulting from Late  
123 Cretaceous inversion of Late Jurassic-Early Cretaceous rift basins during Iberia – Europe  
124 convergence (Salas et al., 2001; Guimerà et al., 2004; Martín-Chivelet et al., 2002). It is divided  
125 into two NW-SE directed branches, the Aragonese and the Castillian branches, separated by the  
126 Tertiary Almazan subbasin (Bond, 1996). The Almazan subbasin is connected to the Duero  
127 basin since the Early Miocene (Alonso-Zarza et al., 2002).

128 The Iberian Range is essentially made of marine carbonates and continental clastic sediments  
129 ranging from Late Permian to Albian, overlying a Hercynian basement. The Cameros subbasin  
130 to the NW represents a late Jurassic-Early Cretaceous trough almost exclusively filled by  
131 continental siliciclastic deposits (Martín-Chivelet et al., 2002 and references therein; Del Rio  
132 et al., 2009). Shortening in the Iberian Range occurred from the Late Cretaceous to the Early  
133 Miocene, along inherited Hercynian NW-SE structures (Gutiérrez-Elorza and Gracia, 1997;  
134 Guimerà et al., 2004; Gutiérrez-Elorza et al., 2002). The opening of the Calatayud basin in the  
135 Aragonese branch occurred during the Early Miocene in response to right-lateral transpression

136 on the southern margin of the Iberian Range (Daroca area) (Colomer and Santanach, 1988). It  
137 is followed during the Pliocene and the Pleistocene, by pulses of extension reactivating faults  
138 in the Calatayud basin, and the formation of grabens such as the Daroca, Munébrega,  
139 Gallocanta, and Jiloca grabens (Fig. 4; Colomer and Santanach, 1988; Gutiérrez-Elorza et al.,  
140 2002; Capote et al., 2002). This is also outlined by the occurrence of Late Pliocene to Early  
141 Pleistocene breccias and glaciais levels in the Daroca and Jiloca grabens (Gracia, 1992, 1993a;  
142 Gracia and Cuchi, 1993; Gutiérrez-Santolalla et al., 1996). These Neogene troughs are filled by  
143 continental deposits and pediments, up to the Quaternary (Fig. 4). The Neogene tectonic pulses  
144 in the Iberian are interrupted by periods of quiescence during which erosion surfaces developed  
145 (Gutiérrez-Elorza and Gracia, 1997).

146 Deformation and uplift of the Iberian Range and Cameros basin resulted in the development of  
147 a new drainage divide between the Duero and Ebro basins and in the isolation of the Almazan  
148 subbasin (Alonso-Zarza et al., 2002). In contrast, the connection between the Duero the Ebro  
149 basins has not been affected by significant deformation and uplift in the proto-Rioja trough  
150 (Mikes, 2010).

151

### 152 2.3 The Rioja trough and Bureba high

153

154 The Rioja trough (Figs. 2, 5) recorded important subsidence, especially during the Cenozoic (>  
155 5 km), related to compression and thrusting on its borders (Jurado and Riba, 1996). As thrusting  
156 initiated in the Pyrenean-Cantabrian belt and in the Iberian Range and Cameros basin, the Rioja  
157 trough became domain of important synorogenic sediment transfer between the Ebro and Duero  
158 basins. During the Paleocene, the Rioja trough was a marine depositional environment. With  
159 the increase of sediment fluxes that originated from the exhumation of surrounding mountain  
160 belts, sedimentation became essentially continental in the Eocene. Thrusting continued during  
161 the Oligocene resulting in the formation of an anticline connecting the Cantabrian domain and  
162 the Cameros inverted basin. This morphologic high (the Bureba anticline, Fig. 5) located in the  
163 center of the area is supposed to have triggered the disconnection between the Duero and Ebro  
164 basins (Mikes, 2010), as suggested by the repartition of alluvial fans on both sides of this  
165 structure (Muñoz-Jiménez and Casas-Sainz, 1997; Villena et al., 1996). During the Miocene,  
166 deformation ceased as evidenced by the deposition of undeformed middle Miocene to Holocene  
167 strata. The Bureba anticline is cored by Albian strata and topped by Santonian limestones and  
168 Oligocene conglomerates controlling the location of the current main drainage divide between  
169 the Ebro and Duero river networks (Fig. 5).

170

## 171 2.4 Climate evolution

172

173 Climate exerts a major control on valley incision, sediment discharge, and on the evolution of  
174 drainage networks (Willet, 1999; Garcia-Castellanos, 2006; Bonnet, 2009; Whipple, 2009;  
175 Whitfield and Harvey, 2012; Stange et al., 2014). The mean annual precipitation map for the  
176 North Iberian Peninsula (Hijmans et al., 2005) shows a similar pattern for both the Ebro and  
177 Duero basins as they record very low precipitation, associated with global subarid conditions,  
178 with the exception of the Cameros basin that record a slightly higher precipitation rate (Fig. 6).  
179 There is a strong contrast to the north, toward the Mediterranean Sea and the most elevated  
180 areas in the Cantabrian and Pyrenean belts, where precipitation drastically increases.

181 The paleoclimatic evolution from the Late Cretaceous to the Neogene is linked both with the  
182 effects of surrounding mountains uplift, and with the latitudinal variation drift of Iberia from  
183 30°N in the Cretaceous to ~40°N during Late Neogene times. The hot-humid tropical climate  
184 of the Late Cretaceous became drier and arid from the Paleocene to the Middle Miocene (López-  
185 Martínez et al., 1986), favouring the development of endorheic lakes (Garcia-Castellanos,  
186 2006). During the Middle-Late Miocene and Early Pliocene, the northern Iberia recorded more  
187 humid and seasonal conditions (Calvo et al., 1993; Alonso-Zarza and Calvo, 2000) with  
188 alternations of cold-wet and hot-dry periods (Bessais and Cravatte, 1988; Rivas-Carballo et al.,  
189 1994; Jiménez-Moreno et al., 2010). More humid and colder conditions took place in the Late  
190 Pliocene, characterized by dry glacial periods and humid interglacials (Suc and Popescu, 2005;  
191 Jiménez-Moreno et al., 2013). Climatic contrasts increased, triggering intense glaciers  
192 fluctuations in the surrounding mountain ranges during the Lower-Middle Pleistocene transition  
193 (1.4-0.8 Ma) (Moreno et al., 2012; Duval et al., 2015; Sancho et al., 2016), and throughout the  
194 Late Pleistocene period, which record glacial / interglacial oscillations, as evidenced by pollen  
195 identification (Suc and Popescu, 2005; Jiménez-Moreno et al., 2010, 2013; Barrón et al., 2016;  
196 García-Ruiz et al., 2016) and speleothem studies (Moreno et al., 2013; Bartolomé et al., 2015).  
197 Glaciers are considered as very efficient erosion tool in continental environment. They are  
198 likely to influence drainage divide migration (Brocklehurst and Whipple, 2002). There is large  
199 evidence of glaciers development especially for the Late Pleistocene in the Pyrenees (Delmas  
200 et al., 2009; Nivière et al., 2016; García-Ruiz et al., 2016), in the Cantabrian belt (Serrano et  
201 al., 2013, 2016; García-Ruiz et al., 2016), and in the Central Range (Palacios et al., 2011, 2012;  
202 García-Ruiz et al., 2016). However, although numerous moraines have been mapped throughout  
203 the Iberian Range (Ortigosa, 1994; García-Ruiz et al., 1998; Pellicer and Echeverría, 2004),

204 there is no evidence of U-shaped valleys and because of the lack of very high elevated massifs  
205 (>2500 m), the occurrence of active ice tongues are considered as limited, if not precluded  
206 (García-Ruiz et al., 2016).

207

### 208 **3. Evidence of divide mobility between the Duero and Ebro catchments**

209

210 The easternmost part of the Duero river is opposed to the Ebro tributaries that are the Jalon,  
211 Huecha, Queiles, Alama, Cidacos, Iregua, and Najerilla rivers, whereas the Arlanzon and  
212 Pisuerga rivers (Duero tributaries) are opposed to the Najerilla, Tiron, Oca, and Rudron rivers,  
213 and to the westernmost part of the Ebro river (Fig. 3). The northeastern part of the Duero basin  
214 (the easternmost Duero river, the Arlanzon and Pisuerga rivers) mainly consists of broad flat  
215 valleys characterized by low incision depth and low-gradient streams with concave longitudinal  
216 profiles (Antón et al., 2012, 2014). By contrast, the western part of the Ebro basin is  
217 characterized by more incised valleys, especially in the Cantabrian and in the Cameros – Iberian  
218 Range domains, with more complex longitudinal profiles (knickpoints, remnants of high  
219 elevated surfaces). Previous studies (Gutiérrez-Santolalla et al., 1996; Pineda, 1997; Mikes,  
220 2010) already shown that the Jalon and Homino rivers, which belong to the Ebro basin, have  
221 recently captured parts of the Duero basin in the Iberian Range and in the Rioja trough,  
222 respectively. Such evolution has been recorded by the occurrence of geomorphological markers  
223 as wind gaps and elbows of captures, as well as by the presence of knickpoints and/or remnants  
224 of high elevated surfaces in river long profiles. To highlight this dynamic evolution, we  
225 performed a morphometric analysis of rivers all around the divide separating the Ebro basin  
226 from the Duero basin, with particular attention given to the Aragonese branch of the Iberian  
227 Range (Fig. 4) and to the Rioja Trough (Fig. 5), where captures have already been described.  
228 The studied basins were digitally mapped using high-resolution (~30 meters) digital elevation  
229 models (DEMs) from SRTM 1 Arc-Second Global elevation data available at the U.S.  
230 Geological Survey ([www.usgs.gov](http://www.usgs.gov)). The different DEMs were assembled using the ENVI  
231 software. We also used 1:50,000 geological maps from the Instituto Geológico y Minero de  
232 España ([www.igme.es](http://www.igme.es)). We used the TopoToolbox, a MATLAB-based software developed by  
233 Schwanghart and Scherler (2014), to extract the river network and longitudinal profiles and the  
234  $\chi$  Analysis Tool developed by Mudd et al. (2014).

235

#### 236 **3.1 Fluvial captures and related knickpoints in the Iberian Range**

237

238 Neogene tectonics in the Iberian range controlled the uplift of topographic ranges and the  
239 formation of several basins whose connection with the Ebro or the Duero has occasionally  
240 changed through time. Nowadays, the western part of the Almazan subbasin (Figs. 2, 4) belongs  
241 to the Duero catchment, its eastern part being drained by the Ebro drainage network and  
242 especially by the Jalon river and its tributaries (Fig. 4). Gutiérrez-Santolalla et al. (1996)  
243 proposed that the Jalon river captured this domain after cutting into the Mesozoic and Neogene  
244 strata and the two Paleozoic ridges of the Aragonese branch of the Iberian Range. They pointed  
245 out several chronostratigraphic evidence that allow them to build a relative chronology of  
246 capture events in the Jalon network history. First, the incision of the northern Paleozoic ridge  
247 and capture of the Calatayud basin by the Jalon river is attributed to a post-Messinian age. The  
248 Jiloca river, the easternmost main Jalon tributary, is then thought to capture the Daroca graben  
249 area to the east during the Late Pliocene – Early Pleistocene. This is followed from the Early to  
250 Late Pleistocene by the capture of the Jiloca graben to the southeast and finally by the capture  
251 of the Munébraga graben to the southwest, by the Jalon river (Gutiérrez-Santolalla et al., 1996),  
252 toward the easternmost part of the Almazan subbasin.

253 The Jalon river and tributaries show knickpoints in their longitudinal profiles (Fig. 4), at  
254 locations that are consistent with the events of captures proposed by Gutiérrez-Santolalla et al.  
255 (1996), suggesting that these captures are actually witnessed by knickpoints. The capture of the  
256 Jiloca graben corresponds to a major knickpoint in the Jiloca river profile that appears very  
257 smoothed, and that is followed by an upstream ~50 km long flat domain preserved at ~1000 m  
258 high above sea level. This imparts a convex shape to the Jiloca profile (Fig. 4). Due to the short  
259 period of time between the formation of the Jiloca graben (the earliest glacial deposits are  
260 attributed to the Middle Pliocene) and its capture (Early Pleistocene; Gutiérrez-Santolalla et al.,  
261 1996), we suggest this upstream domain was a short-lived endorheic domain that has never  
262 been externally drained before being captured by the Ebro network. In the northwestern part of  
263 the Jiloca graben, the Cañamaria river, a tributary of the Jiloca river, heads to the northwest,  
264 reaching the Gallocanta basin, also considered as a former graben (Gracia, 1993b; Gracia et al.,  
265 1999; Gutiérrez-Elorza et al., 2002). The upstream part of its river long profile is characterized  
266 by a sharper knickpoint at the entrance of the basin, and is followed by a ~15 km long flat  
267 domain (Fig. 4). Similarly to the Jiloca graben, the Gallocanta basin appears to be a short-lived  
268 endorheic domain that has been more recently captured by the Jiloca river network.

269 According to Gutiérrez-Santolalla et al. (1996), the Jalon river reached the southern Paleozoic  
270 ridge of the Aragonese branch, to the southwest of the Calatayud basin, captured the Munébraga  
271 graben and the Almazan subbasin (also characterized by a pronounced knickpoint) during the



272 Pleistocene-Holocene, slightly after the capture of the Jiloca graben by the Jiloca river. This is  
273 coherent with morphological analysis of longitudinal profiles, as the major knickpoint related  
274 to the capture of the Jiloca graben appears very smoothed, whereas knickpoints observed in the  
275 west are sharper, suggesting they are younger. However despite a similar bedrock we cannot  
276 ruled out some local influence of the lithology on the shape of these knickpoints.  
277 Finally, the Piedra river (Jalon tributary) long profile shows major sharp knickpoints and two  
278 successive ~30 km long almost flat domains in the Almazan subbasin, at ~900-1000 m above  
279 sea level (Fig. 4). In addition, the upper reach of the river long profiles of the Jalon river, and  
280 of its tributary the Blanco river, are characterized by major sharp knickpoints, and by a ~15 km  
281 long flat domain at ~1000-1100 m above sea level, in the Mesozoic Castilian branch of the  
282 Iberian Range (Fig. 4).

283

### 284 3.2 Fluvial captures and related knickpoints in the Rioja trough area

285

286 In the Rioja trough area, the position of the Ebro-Duero divide is partly controlled by the Bureba  
287 anticline. It consists of folded Middle Cretaceous to Early Miocene series, covered by  
288 undeformed Middle Miocene to Holocene deposits (Fig. 5). The anticline is orientated E-W to  
289 the west and NE-SW to the east. The western part of the Rioja trough to the west of the NE-SW  
290 directed branch of the Bureba anticline (Fig. 5), used to be drained toward the Duero basin since  
291 the Oligocene (Pineda, 1997; Mikes, 2010). The westward migration of the divide to its current  
292 location is thought to have occurred in several steps of captures as shown by the occurrence of  
293 remnants of escarpments during the Late Miocene - Pliocene (Mikes, 2010). Once the eastern  
294 branch of the Bureba anticline has been incised, the Ebro tributaries captured the western part  
295 of the Rioja trough, up to the E-W branch of the Bureba anticline to the southwest, from the  
296 Late Miocene to the Pliocene. The western part of the anticline forms a topographic ridge that  
297 is incised by Jordan river (Fig. 5) in a place where the divide between the Ebro and Duero river  
298 networks is located to the north of the ridge. To the East of this location however, the  
299 topographic ridge formed by the Bureba anticline controls the current location of the main  
300 drainage divide (Fig. 5). Here, the ridge exhibits several wind gaps, located on the northward  
301 prolongation of the Hoz, Rioseras, and Nava Solo rivers (Figs. 5, 7). Further east, the Diabolo  
302 river does not incise the ridge and its headwater is located in the core of the eastern branch of  
303 the Bureba anticline, the Fuente Valley (Fig. 5). These last streams are tributaries of the Ubierna  
304 river, which is a tributary of the Arlanzon river and so, of the Duero river. To the north, the Ebro  
305 river system is represented, from west to east, by the Homino river (a tributary of the Oca river)

306 and its four tributaries, the Molina, the Fuente Monte, the Zorica, and the San Pedro rivers (Figs.  
307 5, 7). All these streams are outlined by Late Pleistocene to Holocene alluvial series that are  
308 deposited at the bottom of their respective valleys. Valleys from the Duero side appears larger  
309 than those from the Ebro side, which are significantly more incised.

310 The Jordan river's headwater is located north of the ridge formed by the Bureba anticline. We  
311 can continuously follow its valley deposits northward along a broadly gentle slope, up to the  
312 locality of Coraegula (Fig. 5). However, the current course of the Jordan river is cut ~8 km  
313 south, in the vicinity of Hontomin, by the Homino (Ebro) river (Figs. 5B, C, 7). This fluvial  
314 capture is characterized by a well-defined and highly incised elbow of capture, already  
315 described by Pineda (1997) and Mikes (2010). The longitudinal profile of the Homino river  
316 shows a sharp knickpoint located on Hontomin (Fig. 7C). Finally, there is a small wind gap on  
317 the divide between the two opposite rivers (Figs. 5, 7).

318 To the southeast, the headwater of the Hoz river is located to the south of a wind gap cut into  
319 the Bureba ridge (Fig. 7C). To the north, in the exact prolongation of the Hoz river, the Molina  
320 river shows a bend similar to the elbow of capture previously described for the Homino river  
321 (Fig. 7) and there is a minor knickpoint located on this elbow, according to the extracted river  
322 long profile. Thus, it is likely that the Molina river used to represent the former upper reach of  
323 the Hoz river, in a period when the Ebro-Duero divide was located northward, before being  
324 captured by the Ebro network.

325 To the east, the Rioseras and the Nava Solo rivers have also their headwater located to the South  
326 of wind gaps in the Bureba ridge (Fig. 7). Similarly, in their exact prolongations, the Fuente  
327 Monte and the Zorica rivers show important elbows of capture with minor knickpoints. They  
328 may also represent former upper reaches of Duero streams that have been captured by the Ebro  
329 network (Figs. 5, 7, 8).

330 Further east, the headwater of the Diablo river is located on the depression represented by the  
331 core of the eastern branch of the Bureba anticline, the Fuente valley. In its prolongation to the  
332 northeast, the San Pedro river incises the northeastern termination of the anticline from the  
333 north before entering the valley, leading to a southward retreat of the divide (Fig. 5). Capture is  
334 again evidenced by important incision contrast between Ebro and Duero systems, and by sharp  
335 knickpoints on the upper reach of the San Pedro river long profile when crossing the Santonian  
336 dolomites (Fig. 8). According to this whole set of observations, and in agreement with previous  
337 findings of Pineda (1997) and Mikes (2010), we propose that the western part of the Rioja  
338 trough, in the Bureba area has been recently captured by the Ebro drainage network leading to

339 a sequence of southwestward retreat of the main drainage divide, toward the Duero basin (Fig.  
340 7E).

341

342 A similar capture pattern can be observed further west in the continuity of the Bureba anticline  
343 (Fig. 5). The San Anton river shows a well-defined elbow of capture accompanied by a  
344 smoothed knickpoint (See Fig. S1 in the Supplement) at its junction with the Rudron river (Ebro  
345 tributary). The river course is highly incised toward the east, along the northern flank of the  
346 WNW – ESE anticline, almost connecting to the upper reach of the Ubierna river. Valley  
347 deposits are also observed in the continuity of the Ubierna valley, which former route is  
348 suggested by a wind gap (Fig. 5). However, this domain is no longer connected to its network  
349 as it is now wandered from the North by the Nava river, a tributary of the Moradillo river, which  
350 is a tributary of the Rudron river. This domain clearly records captures leading to divide  
351 migration toward the Duero, also in favor of the Ebro basin.

352

353 3.3 Past position of the Ebro-Duero divide and implication for stream-power of the Duero River

354

355 We used all observations that support divide migration in the Iberian Range and Rioja trough  
356 to estimate a paleo-position of the drainage divide between the Duero and Ebro drainage basins  
357 (Fig. 9). For this purpose, we considered the location of major knickpoint along the rivers where  
358 fluvial captures are defined. Both the Ebro river and several tributaries show high elevated ~10-  
359 20 km long flat domains at ~800 – 1200 m a.s.l. and major knickpoints in the upper reach of  
360 their long profiles as the Rudron, Queiles, and Alama rivers, as well as the Homino river and  
361 its tributaries: the Puerta Nogales and Valdelanelala rivers (Figs. 5, 8; Fig. S1). All these flat  
362 domains may not be related to surface uplift as they are not clearly associated with active  
363 tectonic features. The Duero basin being characterized by a high mean elevation (~1000 m) and  
364 by a very limited incision in the vicinity of the Ebro/Duero drainage divide, a sudden divide  
365 migration toward the Duero basin is then expected to isolate such high elevated and relatively  
366 preserved surfaces. We suggest these flat domains have been recently captured by Ebro  
367 tributaries, and represent remnants of Duero drainage areas, integrated into the Ebro catchment  
368 from divide retreat toward the Duero basin. Overall, we consider a paleodrainage divide  
369 delimited by these high-elevated knickpoints and flat domains, except for the Jiloca graben area  
370 to the southeast, characterized by the occurrence of short-lived endorheic domains (Fig. 9).

371 Incision in the Ebro basin leads to the capture of new drainage areas, whereas the Duero basin  
372 recorded important loss of its own surface. The present day drainage area of the Cenozoic Duero

373 basin, upstream of the major knickzone observed to the west in the Iberian Massif is ~63000  
374 km<sup>2</sup>. We used the paleo-divide position shown in Figure 9 to define a « recent » captured area  
375 that used to belong to the Duero basin. This area represents ~7700 km<sup>2</sup>, which corresponds to  
376 ~12% of the present-day Cenozoic Duero basin drainage area. Such a reduction of the drainage  
377 area could have strong implications on the evolution of the Duero basin, as important lowering  
378 of water and sediment fluxes, and so of incision throughout the basin. To better resolve the  
379 impact of such drainage area reduction on incision capacity, we perform a stream power analysis  
380 of the Duero river. We consider the specific stream power,  $\omega$ , defined as  $\omega = \rho g Q S / W$ , where  
381  $\rho$  is water density,  $g$  is gravitational acceleration,  $Q$  is discharge,  $S$  is local river gradient, and  
382  $W$  is river width (see the Supplement for details of the calculation). We calculate  $\omega$  for the  
383 present-day Duero river, and for a restored ancient Duero river that drained this 12% of lost  
384 area. We plot the difference (ancient – present day) between the two curves in Figure 10, with  
385 the Duero river long profile. Calculated difference in specific stream power values are relatively  
386 low ( $< 2 \text{ W m}^{-2}$ ) for the upstream part of the basin, but increase to  $\sim 5 \text{ W m}^{-2}$  when approaching  
387 the major knickzone at a distance of  $\sim 350 \text{ km}$  from the river mouth. The knickzone is  
388 characterized by peak values exceeding  $10 \text{ W m}^{-2}$ , which rapidly decrease to  $\sim 0 \text{ W m}^{-2}$  at the  
389 base of the knickzone ( $\sim 200 \text{ km}$ ) and up to the river mouth (Fig. 10). Some alternating peak  
390 and null values are observed in the lower reach of the river and may be related to the occurrence  
391 of numerous dams along the river. Overall, the specific stream power calculated for the ancient  
392 Duero river show higher values than for the present day from the base of the knickzone to the  
393 uppermost reach of the river (Fig. 10). This implies a general decrease of the Duero river's  
394 incision capacity between this ancient state to the present day, magnified on the knickzone.

395

### 396 3.4 $\chi$ map

397

398 The comparison of the shape of longitudinal profiles of rivers across divide is a way that has  
399 been proposed recently to infer disequilibrium between rivers and the potential migration of  
400 their divide (Willett et al., 2014). Although the slope-area analysis of channel profiles (e.g.  
401 Whipple and Tucker, 1999; Kirby and Whipple, 2012) is potentially a powerful tool to evidence  
402 differences in the equilibrium state of rivers across divide, and then to infer their migration  
403 (Willett et al., 2014), this method is limited and even biased by the quality of the topographic  
404 data. Indeed, both a low-resolution of the DEM and corrections brought to the DEM (filling or  
405 carving), lead to substantial uncertainties that are automatically transferred to the slope-area  
406 data. To avoid slope measurements, Perron and Royden (2012) proposed a procedure based on

407 a coordinate transformation allowing linearizing river profiles. Considering constant uplift rate  
408 (U) and erodibility (K) in time and space the  $\chi$ -transformed profile of a river is defined by the  
409 following equation (Perron and Royden, 2012; Mudd et al., 2014):

410

$$411 \quad z(x) = z_b(x_b) + \left(\frac{U}{KA_0^m}\right)^{1/n} \chi$$

412

413 with

$$414 \quad \chi = \int_{x_b}^x \left(\frac{A_0}{A(x)}\right)^{\frac{m}{n}} dx$$

415 where  $z(x)$  is the elevation of the channel,  $x$  is the longitudinal distance,  $z_b$  is the elevation at  
416 the river's base level (distance  $x_b$ ),  $A$  is the drainage area,  $A_0$  is a reference drainage area, and  
417 exponents  $m$  and  $n$  are empirical constants.

418

419 When using the  $\chi$  variable instead of the distance for plotting the elevation  $z$  along channel, ( $\chi$ -  
420 plot), the longitudinal profile of a steady-state channel is shown as a straight line (Perron and  
421 Royden, 2012). Any channel pulled away from this line is in disequilibrium and is then expected  
422 to attempt to reach equilibrium. Mapping  $\chi$  on several watersheds and comparing  $\chi$  across  
423 drainage divides is then a potential way to high disequilibrium between rivers across divide and  
424 to elucidate divide migration and drainage reorganization through captures (Willett et al., 2014).  
425 We used the  $\chi$  Analysis Tool developed by Mudd et al. (2014) to select the best  $m/n$  ratio by  
426 iteration (Perron and Royden, 2012) and to calculate  $\chi$  for rivers throughout the divide between  
427 the Ebro and Duero basins from a similar base level at 850 m a.s.l. The best mean  $m/n$  ratio for  
428 all our streams is 0.425, which falls in the typical range of values observed for rivers ( $\sim 0.4 -$   
429  $0.6$ : e.g. Kirby and Whipple, 2012). The resulting map (Fig. 11) shows  $\chi$  values calculated on  
430 different opposite streams in the vicinity of the Ebro/Duero drainage divide. Similar values on  
431 both sides of the divide suggest the two opposite streams are at equilibrium, whereas strong  
432 contrasted  $\chi$  values imply disequilibrium leading to divide migration, continuously or through  
433 fluvial capture, toward the high  $\chi$  values (Willett et al., 2014). The map of  $\chi$  values actually  
434 shows significant contrasting values across the Ebro/Duero divide. We comment here these  
435 contrasts along the divide from the SE to the NW of the area considered (Fig. 11).

436 There is a strong contrast in  $\chi$  values between the headwater of the Jalon river (Fig. 11),  
437 characterized by low values ( $\sim 300$  m), and the closest part from the divide of the Bordecorex  
438 river (Fig. 4), a tributary of the Duero river ( $\sim 500$  m). Such a disequilibrium implies divide

439 migration toward the Duero basin, predicting the capture of the uppermost reach of the  
440 Bordecorex river by the Jalon river. To the north, tributaries of the Jalon river show slightly  
441 lower  $\chi$  values than the tributaries of the Duero river. This suggests a relative stable situation  
442 although small captures may occur toward the Duero basin. A higher contrast is observed  
443 around the easternmost part of the Duero basin, which is surrounded by the Ebro basin. The  
444 Araviana river (tributary of the Duero river) seems to be taken in a bottleneck between the  
445 Manubles river to the south and the Queiles river to the north (Fig. 4), which both show lower  
446  $\chi$  values (Fig. 11). Toward the east, there is a strongest  $\chi$  values contrast between headwaters  
447 of the Araviana river (>700 m) and of the Isuela (Jalon tributary) and Huecha rivers (<100 m).  
448 This domain appears clearly in disequilibrium and is expected to be captured by the Ebro  
449 drainage network. Such high  $\chi$  values differences appear also to the northwest (Fig. 11), in the  
450 southern part of the Cameros basin where the Duero river and its tributaries' headwaters show  
451  $\chi$  values >500-700 m, whereas the facing rivers (Alama, Cidacos, Iregua, and Najerilla) are all  
452 characterized by low  $\chi$  values <100 m. This predicts important disequilibrium and divide  
453 migration and fluvial captures toward the south. Northwestward,  $\chi$  values between Duero and  
454 Ebro network are more similar indicating that the divide is relatively more stable here, up to the  
455 westernmost part of the Ebro basin (Fig. 11). However, there are some slight localized  $\chi$  value  
456 contrasts (~200 / ~450 m) as observed between the Tiron and the Arlanzon rivers, between the  
457 Rudron and the Ubierna and Urbel rivers, and between the Ebro and the Pisuerga rivers (Fig.  
458 11). It suggests minor local captures toward the Duero basin.

459  
460 To sum up,  $\chi$  values calculated in the vicinity of the drainage divide between the Ebro and  
461 Duero river networks show a general disequilibrium (Fig. 11) as the Ebro network is  
462 characterized by low  $\chi$  values (up to ~200-300 m) compared to those for the Duero network  
463 (up to ~450-700 m). In complement with all the evidence of divide displacements induced by  
464 captures described previously this allows predicting a general divide migration toward the  
465 Duero basin through headwater retreat, in favor of the Ebro tributaries, especially around the  
466 Almazan subbasin, which is expected to be entirely captured by the Ebro basin.

467

## 468 **4. Discussion**

469

### 470 4.1 Long term trend of divide migration

471

472 The oldest capture evidence in our study area corresponds to the incision of the northern part  
473 of the Iberian Range by the Jalon river and by the capture of the Calatayud basin, attributed to  
474 the post-Messinian (Gutiérrez-Santolalla et al. 1996). We propose, based on morphological  
475 evidence (Fig. 4) and in agreement with stratigraphic data (Gutiérrez-Santolalla et al. 1996),  
476 that the Jalon river system captured the Jiloca graben to the east since the Early Pleistocene,  
477 before progressively capturing the Almazan subbasin toward the west in the Holocene  
478 (Gutiérrez-Santolalla et al. 1996). From  $\chi$  analysis (Fig. 11), we deduce that the eastern part of  
479 the Duero basin, the Almazan subbasin, is being actively captured by Ebro tributaries that  
480 drained the Iberian Range and the Cameros basin. Despite low contrasts in  $\chi$  values, local  
481 captures are also suggested in the vicinity of the Ebro / Duero drainage divide toward the  
482 northwest. Capture is further implied by the occurrence of numerous high elevated (~1000 m)  
483 knickpoints and low-relief surfaces (Figs. 5, 8, 9, 11).

484 Thus, there is a good correlation between  $\chi$  predictions and morphological and stratigraphic  
485 data implying long-lasting captures and divide migration during Pliocene, Pleistocene, and  
486 Holocene times in favor of the Ebro basin.

487

488 The pursuit of such a long-term capture trend may be driven by tectonic and/or climatic forcing  
489 (Willett, 1999; Montgomery et al., 2001; Sobel et al., 2003; Sobel and Strecker, 2003; Bonnet,  
490 2009; Whipple, 2009; Castelltort et al., 2012; Kirby and Whipple, 2012; Goren et al., 2015; Van  
491 der Beek et al., 2016). However, such long-term trend in drainage reorganization may also occur  
492 in tectonically quiescent domains, independently of external forcing (Prince et al., 2011). Here,  
493 the Iberian Range and the Cameros basin recorded extension pulses from the Late Miocene to  
494 the Early Pleistocene, responsible for the formation of several grabens as previously described  
495 (Gutiérrez-Santolalla et al., 1996; Capote et al., 2002). Extension events are also recorded  
496 during the Holocene, nevertheless, the youngest erosion surface of Late Pliocene-Early  
497 Pleistocene age observed in our study area shows no tectonic-related deformation and  
498 reworking, suggesting that tectonic activity is reduced here (Gutiérrez-Elorza and Gracia,  
499 1997). This is also consistent with the relative scarcity of seismic activity observed in our study  
500 area, compared, for instance, to the Pyrenees, or to the Betics (Herraiz et al., 2000; Lacan and  
501 Ortuño, 2012). We consequently propose that local tectonic activity is not the main driver of  
502 the capture histories documented here, as most capture events postdate the cessation of tectonic  
503 activity, and occur during periods of quiescence (Gutiérrez-Santolalla et al., 1996).

504

505 The Cameros Massif is characterized by relatively high mean annual precipitation up to ~1000  
506 mm/an (Fig. 6) with high elevation (~1400-2200 m) in comparison with the surrounding areas.  
507 This contrasts with the adjacent Ebro and Duero basins where low precipitation rates, of ~400-  
508 500 mm/an (Hijmans et al., 2005), illustrate subarid climate conditions. The Cameros area is  
509 the only place in our study area where a contrast in precipitation pattern (Fig. 6) would  
510 potentially drive a migration of the divide toward the drier, Duero area. Given that the same  
511 pattern is observed everywhere, even where there isn't any precipitation difference, we suggest  
512 that the present day climatic condition is unlikely to control the general pattern of current  
513 drainage reorganization between the Ebro and Duero basins. During the Pliocene and the  
514 Pleistocene, the climatic record in the northern Iberian Peninsula is characterized by alternations  
515 between similar subarid conditions and intense glaciation. However, there is no clear evidence  
516 of important glacier development and related erosion in our study area, especially for the  
517 Cameros basin and the Iberian Range (Ortigosa, 1994; García-Ruiz et al., 1998, 2016; Pellicer  
518 and Echeverría, 2004). This indicates that drainage evolution between the Ebro and Duero  
519 basins is unlikely to be related to climatic evolution.

520

521 4.2 Excavation of the Ebro basin as the main factor controlling divide migration and limiting  
522 incision of the Duero river

523

524 A striking morphological feature for river capture in our study area is the important contrast in  
525 the incision pattern (e.g. Fig. 1B) from one side of the divide to the other. This suggests that the  
526 incision capacity of the river network is the main driver for capture and divide migration. Both  
527 tectonic and climatic forcing does not appear to control drainage reorganization between the  
528 Ebro and Duero basins.

529 The opening of the Ebro basin toward the Mediterranean Sea during the Late Miocene led to  
530 widespread excavation (García-Castellanos et al., 2003, García-Castellanos and Larrasoána,  
531 2015), favored by more humid and seasonal climatic conditions (Calvo et al., 1993; Alonso-  
532 Zarza and Calvo, 2000). By contrast, incision related to the opening of the Duero basin toward  
533 the Atlantic Ocean is concentrated to the west in the Iberian Massif, characterized by a  
534 largescale knickzone (150 km long and 500 m high) in the Duero river long profile (Fig. 1B).  
535 This contrasts with the limited eastward propagation of incision in the Cenozoic part of the  
536 basin (Antón et al., 2012, 2014), despite climatic conditions similar to the Ebro basin. An  
537 explanation resides in the fact that the resistant Iberian Massif basement rocks may have  
538 controlled and limited incision and drainage reorganization in the Cenozoic Duero basin (Antón



539 et al., 2012). The Duero profile upstream of this major knickzone may be considered as a high  
540 elevated local base level for its tributaries there. Difference between the Ebro and Duero base-  
541 levels implies a major contrast in fluvial dynamics. We suggest the systematic and long-term  
542 trend of divide migration toward the Duero basin and fluvial capture in favor of the Ebro basin  
543 is driven by the differential incision behavior, controlled by base-level difference.

544 Our stream power analysis along the Duero river (Fig. 10) shows that the difference in drainage  
545 area of the Duero inferred from our paleo-divide map (Fig. 9) induces a noticeable decrease of  
546 stream power values of the Duero in the vicinity of the knickzone. This stream power is a  
547 minimum estimate because calculation does not take into account possible captures and divide  
548 migration in other areas along the Duero basin divide, nor the full history of the divide migration  
549 through time and the related ongoing decrease in water discharge as documented in laboratory-  
550 scale landscape experiments (Bonnet, 2009). Some contrasts of incision are also observed in  
551 the Iberian Range along the southern border of the Duero, and in the Cantabrian domain to the  
552 North. Both show more important incision than in the Duero basin, suggesting potential river  
553 captures and divide migration at the expense of the Duero basin, increasing the total of lost  
554 drainage area. Even if it gives minimal estimate, our stream power analysis suggests that  
555 drainage area reduction may have limited the erosion in the Duero basin. This provides an  
556 explanation for the preservation of the lithologic barrier to the west, along the main knickzone  
557 of the Duero considered as an intermediate, local base level (Antón et al., 2012). We propose  
558 that the reduction of the Duero drainage area caused by captures and incision in the Ebro basin,  
559 is responsible for a significant decrease of the incision capacity in the Duero basin. We infer  
560 that the ongoing drainage network growth in the Ebro basin may be responsible for the current  
561 preservation of large morphological relicts of the-endorheic stage in the Duero basin.

562 The opening of the Ebro basin toward the Mediterranean Sea resulted in a drastic base level  
563 drop. This results in the establishment of an upstream-migrating incision wave that propagates  
564 to every tributary of the Ebro network, responsible for knickpoints migration (Schumm et al.,  
565 1987; Whipple and Tucker, 1999; Yanites et al., 2013) and for drainage reorganization and  
566 divide migration. The  $\chi$  analysis that we performed along the current Ebro-Duero divide (Fig.  
567 11) highlights areas where geomorphic disequilibrium is still ongoing, which suggests that they  
568 are areas where divide is currently mobile. The modelling study performed by Garcia-  
569 Castellanos and Larrasoña (2015) suggests that the re-opening of the Ebro basin occurred  
570 between 12.0 and 7.5 Ma. This indicates that the growth of the drainage network of the Ebro  
571 basin and the establishment of new steady-state conditions is a long-lived phenomenon, which  
572 is still not achieved today.

573

574 **Conclusion**

575

576 In this paper we present a morphometric analysis of the landscape along the divide between the  
577 Ebro and Duero drainage basins located in the northern part of the Iberian Peninsula. This area  
578 shows numerous evidence of river captures by the Ebro drainage network resulting in a long-  
579 lasting migration of their divide, toward the Duero basin. Although these two basins record a  
580 similar geological history, with a long endorheic stage during Oligocene and Miocene times,  
581 they show a very contrasted incision and preservation state of their original endorheic  
582 morphology. Since the Late Miocene, the Ebro basin was opened to the Mediterranean Sea and  
583 record important erosion. On the opposite, the Duero was opened to the Atlantic Ocean since  
584 the Late Miocene – Early Pliocene but its longitudinal profile exhibits a pronounced knickpoint,  
585 which delimits an upstream domain of low relief and limited incision, likely representing a  
586 relict of its endorheic topography. We propose that this contrast of incision is the main driver  
587 of the migration of divide that we document. The morphological analysis of rivers across the  
588 divide highlights areas where geomorphic disequilibrium is still ongoing, which suggests that  
589 the Ebro-Duero divide is currently mobile. The quantification of the decrease of the drainage  
590 area of the Duero based on the reconstruction of a paleo-position of the Ebro-Duero divide  
591 shows that the divide migration results in a significant lowering of the stream power of the  
592 Duero river, particularly along its knickzone. We suggest that divide migration induces a  
593 decrease of the incision capacity of the Duero river, thus favoring the preservation of large  
594 relicts of the endorheic morphology in the upstream part of this basin.

595

596

597 **Author contributions**

598 AV undertook morphometric modeling and interpretation, and wrote the paper. SB and FM  
599 contributed to the interpretation and the writing.

600

601

602 **Competing interests.**

603 The authors declare that they have no conflict of interest.

604

605 **Acknowledgements.**

606 This study was funded by the OROGEN Project, a TOTAL-BRGM-CNRS consortium. We  
607 thank two reviewers and associated Editor Veerle Vanacker for very useful and constructive  
608 comments that greatly helped us to clarify and improve this manuscript.

609

610

## 611 References

612

613 Alonso-Zarza, A. M. and Calvo, J. P.: Palustrine sedimentation in an episodically subsiding  
614 basin: the Miocene of the northern Teruel Graben (Spain), *Palaeogeog., Palaeoclimatol.,*  
615 *Palaeoecol.*, 160, 1-21, 2000.

616

617 Alonso-Zarza, A. M., Armenteros, I., Braga, J. C., Muñoz, A., Pujalte, V., Ramos, E., Aguirre,  
618 J., Alonso-Gavilán, G., Arenas, C., Ignacio Baceta, J., Carballeira, J., Calvo, J. P., Corrochano,  
619 A., Fornós, J. J., González, A., Luzón, A., Martín, J. M., Pardo, G., Payros, A., Pérez, A., Pomar,  
620 L., Rodriguez, J. M., and Villena, J.: Tertiary, in: *The Geology of Spain*, Gibbons, W. and  
621 Moreno, T. (Eds.): The Geological Society, London, 293-334, 2002.

622

623 Antón, L., Rodés, A., De Vicente, G., Pallàs, R., Garcia-Castellanos, D., Stuart, F. M., Braucher,  
624 R., and Bourlès, D.: Quantification of fluvial incision in the Duero Basin (NW Iberia) from  
625 longitudinal profile analysis and terrestrial cosmogenic nuclide concentrations, *Geomorph.*,  
626 165-166, 50-61, <https://doi.org/10.1016/j.geomorph.2011.12.036>, 2012.

627

628 Antón, L., Rodés, A., De Vicente, G., and Stokes, M.: Using river long profiles and geomorphic  
629 indices to evaluate the geomorphological signature of continental scale drainage capture, Duero  
630 basin (NW Iberia), *Geomorph.*, 206, 250-261, <https://doi.org/10.1016/j.geomorph.2013.09.028>,  
631 2014.

632

633 Babault, J., Loget, N., Van Den Driessche, J., Castelltort, S., Bonnet, S., and Davy, P.: Did the  
634 Ebro basin connect to the Mediterranean before the Messinian salinity crisis ?, *Geomorph.*, 81,  
635 155-165, <https://doi.org/10.1016/j.geomorph.2006.04.004>, 2006.

636

637 Barrón, E., Postigo-Mijarra, J. M., and Casas-Gallego, M.: Late Miocene vegetation and climate  
638 of the La Cerdanya Basin (eastern Pyrenees, Spain), *Rev. Palaeobot. Palynol.*, 235, 99-119,  
639 <https://doi.org/10.1016/j.revpalbo.2016.08.007>, 2016.

640

641 Bartolomé, M., Sancho, C., Moreno, A., Oliva-Urcia, B., Belmonte, Á., Bastida, J., Cheng, H.,  
642 and Edwards, R. L.: Upper Pleistocene interstratal piping-cave speleogenesis: The Seso Cave  
643 System (Central Pyrenees, Northern Spain), *Geomorph.*, 228, 335-344,  
644 <https://doi.org/10.1016/j.geomorph.2014.09.007>, 2015.

645

646 Bessais, E. and Cravatte, J.: Les écosystèmes végétaux Pliocènes de Catalogne Méridionale.  
647 Variations latitudinales dans le domaine Nord-Ouest Méditerranéen, *Geobios*, 21, 49-63, 1988.

648

649 Bond, J.: Tectono-sedimentary evolution of the Almazan Basin, NE Spain, in: Friend, F. and  
650 Dabrio, C. (Eds.): *Tertiary Basins of Spain: the Stratigraphic Record of Crustal Kinematics*,  
651 *World and Regional Geology*, 6, Cambridge University Press, Cambridge, 203-213, 1996.

652

653 Bonnet, S.: Shrinking and splitting of drainage basins in orogenic landscapes from the migration  
654 of the main drainage divide, *Nat. Geosc.*, 90, 766-771, <https://doi.org/10.1038/NGEO666>,  
655 2009.

656

657 Brocklehurst, S. H. and Whipple, K. X.: Glacial erosion and relief production in the Eastern  
658 Sierra Nevada, California, *Geomorph.*, 42, 1-24, 2002.

659

660 Calvo, J. P., Daams, R., and Morales, J.: Up-to-date Spanish continental Neogene synthesis and  
661 paleoclimatic interpretation. *Revista de la Sociedad Geologica de España*, 6, 29-40, 1993.

662

663 Comeselle, A.J., Urgeles, R., De Mol, B., Camerlenghi, A., and Canning, J.C., Late Miocene  
664 sedimentary architecture of the Ebro Continental Margin (Western Mediterranean; Implications  
665 for the Messinian Salinity Crisis. *Int. J. Earth Sci.*, 103, 423-440, 2014.

666

667 Capote, R., Muñoz, J. A., Simón, J. L., Liesa, C. L., and Arlegui, L. E.: Alpine tectonics 1: the  
668 Alpine system north of the Betic Cordillera, in: *The Geology of Spain*, Gibbons, W. and  
669 Moreno, T. (Eds.): *The Geological Society*, London, 367-400, 2002.

670

671 Castelltort, S., Goren, L., Willett, S. D., Champagnac, J. D., Herman, F., and Braun, J.: River  
672 drainage patterns in the New Zealand Alps primarily controlled by plate tectonic strain. *Nat.*  
673 *Geosci.*, 5, 744–748, <https://doi.org/10.1038/ngeo1582>, 2012.

674

675 Colomer i Busquets, M., and Santanach i Prat, P.: Estructura y evolucion del borde sur-  
676 occidental de la Fosa de Calatayud-Daroca, *Geogaceta*, 4, 29-31, 1988.

677

678 Coney, P. J., Muñoz, J. A., McClay, K. R., and Evenchick, C. A.: Syntectonic burial and post-  
679 tectonic exhumation of the southern Pyrenees foreland fold-thrust belt, *J. Geol. Soc. London*,  
680 153, 9-16, <https://doi.org/10.1144/gsjgs.153.1.0009>, 1996.

681

682 Costa, E., Garcés, M., López-Blanco, M., Beamud, E., Gómez-Paccard, M., and Larrasoaña, J.  
683 C.: Closing and continentalization of the South Pyrenean foreland basin (NE Spain):  
684 magnetochronological constraints, *Basin Res.*, 22, 904-917, <https://doi.org/10.1111/j.1365-2117.2009.00452.x>, 2010.

686

687 Delmas, M., Calvet, M., and Gunnell, Y.: Variability of Quaternary glacial erosion rates – A  
688 global perspective with special reference to the Eastern Pyrenees, *Quat. Sci. Rev.*, 28, 484-498,  
689 <https://doi.org/10.1016/j.quascirev.2008.11.006>, 2009.

690

691 Del Rio, P., Barbero, L., and Stuart, F. M.: Exhumation of the Sierra de Cameros (Iberian Range,  
692 Spain): constraints from low-temperature thermochronologie, in: Liesker, F., Ventura, B., and  
693 Glasmacher, U. A. (Eds.): *Thermochronological Methods: From Palaeotemperature Constraints*  
694 *to Landscape Evolution Models*, Geological Society, London, Special Publications, 324, 154-  
695 166, <https://doi.org/10.1144/SP324.12>, 2009.

696

697 De Vicente, G., Vegas, R., Muñoz, M. A., Silva, P. G., Andriessen, P., Cloetingh, S., González-  
698 Casado, J. M., Van Wees, J. D., Álvarez, J., Carbó, A., and Olaiz, A.: Cenozoic thick-skinned  
699 deformation and topography evolution of the Spanish Central System, *Glob. Planet. Change*,  
700 58, 335-381, <https://doi.org/10.1016/j.gloplacha.2006.11.042>, 2007.

701

702 Duval, M., Sancho, C., Calle, M., Guilarte, V., and Peña-Monné, J. L.: On the interest of using  
703 the multiple center approach in ESR dating of optically bleached quartz grains: Some examples  
704 from the Early Pleistocene terraces of the Alcanadre River (Ebro basin, Spain), *Quat.*  
705 *Geochronol.*, 29, 58-69, <https://doi.org/10.1016/j.quageo.2015.06.006>, 2015.

706

707 Fillon, C. and Van der Beek, P.: Post-orogenic evolution of the southern Pyrenees: constraints  
708 from inverse thermo-kinematic modelling of low-temperature thermochronology data, *Basin*  
709 *Res.*, 23, 1-19, <https://doi.org/10.1111/j.1365-2117.2011.00533.x>, 2012.  
710

711 Fillon, C., Gautheron, C., and Van der Beek, P.: Oligocene-Miocene burial and exhumation of  
712 the Southern Pyrenean foreland quantified by low-temperature thermochronology, *J. Geol. Soc.*  
713 *London*, 170, 67-77, <https://doi.org/10.1144/jgs2012-051>, 2013.  
714

715 Garcia-Castellanos, D.: Long-term evolution of tectonic lakes: Climatic controls on the  
716 development of internally drained basins, *Geol. Soc. Am., Spec. Paper*, 398, 283-294,  
717 [https://doi.org/10.1130/2006.2398\(17\)](https://doi.org/10.1130/2006.2398(17)), 2006.  
718

719 Garcia-Castellanos, D. and Larrasoaña, J. C.: Quantifying the post-tectonic topographic  
720 evolution of closed basins: The Ebro basin (northeast Iberia), *Geology*, 43, 663-666,  
721 <https://doi.org/10.1130/G36673.1>, 2015.  
722

723 Garcia-Castellanos, D., Vergés, J., Gaspar-Escribano, J., and Cloething, S.: Interplay between  
724 tectonics, climate, and fluvial transport during the Cenozoic evolution of the Ebro Basin (NE  
725 Iberia), *J. Geophys. Res.*, 108, 2347, <https://doi.org/10.1029/2002JB002073>, 2003.  
726

727 García-Ruiz, J. M., Ortigosa, L. M., Pellicer, F., and Arnáez, J.: Geomorfología glacial del  
728 Sistema Ibérico, in: Gómez-Ortiz, A. and Pérez-Alberti, A. (Eds.): *Las huellas glaciares de las*  
729 *montañas españolas*, Universidad de Santiago de Compostela, 347-381, 1998.  
730

731 García-Ruiz, J. M., Palacios, D., González-Sampériz, P., De Andrés, N., Moreno, A., Valero-  
732 Garcés, B., and Gómez-Villar, A.: Mountain glacier evolution in the Iberian Peninsula during  
733 the Younger Dryas, *Quat. Sci. Rev.*, 138, 16-30,  
734 <https://doi.org/10.1016/j.quascirev.2016.02.022>, 2016.  
735

736 Goren, L., Castelltort, S., and Klinger, Y.: Modes and rates of horizontal deformation from  
737 rotated river basins: Application to the Dead Sea fault system in Lebanon, *Geology*, 43, 843-  
738 846, <https://doi.org/10.1130/G36841.1>, 2015.  
739

740 Gracia, F. J.: Tectonica pliocena de la Fosa de Daroca (prov. De Zaragoza), *Geogaceta*, 11, 127-  
741 129, 1992.

742

743 Gracia, F. J.: Evolucion cuaternaria del rio Jiloca (Cordillera Iberica Central), in: Fumanal, M.  
744 P. and Bernabeu, J. (Eds.): *Estudios sobre Cuaternario, Medios Sedimentarios, Cambios*  
745 *Ambientales, Habitat Humano*, Valencia, 43-51, 1993a.

746

747 Gracia, F. J.: Evolucion geomorfologica de la region de Gallocanta (Cordillera Iberica Central),  
748 *Geographicalia*, 30, 3-17, 1993b.

749

750 Gracia, F. J., Gutiérrez-Santolalla, F., and Gutiérrez-Elorza, M.: Evolucion geomorfologica del  
751 polje de Gallocanta (Cordillera Ibérica), *Revista Sociedad Geologica de España*, 12, 351-368,  
752 1999.

753

754 Gracia, F. J. and Cuchi, J. A.: Control tectonico de los travertinos fluviales del rio Jiloca  
755 (Cordillera Ibérica), in: *El Cuaternario en España y Portugal*, Actas 2a Reun. Cuat. Ibérico,  
756 *AEQUA y CTPEQ*, Madrid-1989, 2, 697-706, 1993.

757

758 Guimerà, J., Mas, R., and Alonso, Á: Intraplate deformation in the NW Iberian Chain: Mesozoic  
759 extension and Tertiary contractional inversion, *J. Geol. Soc. London*, 161, 291-303,  
760 <https://doi.org/10.1144/0016-764903-055>, 2004.

761

762 Gutiérrez-Elorza, M. and Gracia, F. J.: Environmental interpretation and evolution of the  
763 Tertiary erosion surfaces in the Iberian Range (Spain), in: Widdowson, M. (Ed.):  
764 *Palaeosurfaces: Recognition, Reconstruction and Palaeoenvironmental Interpretation*,  
765 *Geological Society Special Publication*, 120, 147-158, 1997.

766

767 Gutiérrez-Elorza, M., García-Ruiz, J. M., Goy, J. L., Gracia, F. J., Gutiérrez-Santolalla, F.,  
768 Martí, C., Martín-Serrano, A., Pérez-González, A., and Zazo, C.: Quaternary, in: *The Geology*  
769 *of Spain*, Gibbons, W. and Moreno, T. (Eds.): *The Geological Society*, London, 335-366, 2002.

770

771 Gutiérrez-Santolalla, F., Gracia, F. J., and Gutiérrez-Elorza, M.: Consideraciones sobre el final  
772 del relleno endorreico de las fossa de Calatayud y Teruel y su paso al exorreismo. Implicaciones  
773 morfoestratigraficas y estructurales, in : Grandal d'Ánglade, A. and Pagés-Valcarlos, J. (Eds.) :

774 IV Reunion de Geomorfologia, Sociedad Española de Geomorfologia, O Castro (A Coruña),  
775 23-43, 1996.  
776

777 Herraiz, M., De Vicente, G., Lindo-Ñaupari, R., Giner, J., Simón, J. L., González-Casado, J.  
778 M., Vadillo, O., Rodríguez-Pascua, M. A., Cicuéndez, J. I., Casas, A., Cabañas, L., Rincón, P.,  
779 Cortés, A. L., Ramírez, M., and Lucini, M.: *Tectonics*, 19, 762-786, 2000.  
780

781 Hijmans, R. J., Cameron, S. E., Parra, J. L., Jones, P. G., and Jarvis, A.: Very high resolution  
782 interpolated climate surfaces for global land areas, *Int. J. Climatol.*, 25, 1965-1978,  
783 <https://doi.org/10.1002/joc.1276>, 2005.  
784

785 Jiménez-Moreno, G., Fauquette, S., and Suc, J. P.: Miocene to Pliocene vegetation  
786 reconstruction and climate estimates in the Iberian Peninsula from pollen data, *Rev. Palaeobot.*  
787 *Palynol.*, 162, 403-415, <https://doi.org/10.1016/j.revpalbo.2009.08.001>, 2010.  
788

789 Jiménez-Moreno, G., Burjachs, F., Expósito, I., Oms, O., Carrancho, Á., Villalaín, J. J., Agustí,  
790 J., Campeny, G., Gómez de Soler, B., and Van der Made, J.: Late Pliocene vegetation and  
791 orbital-scale climate changes from the western Mediterranean area, *Global Planet. Change*, 108,  
792 15-28, <https://doi.org/10.1016/j.gloplacha.2013.05.012>, 2013.  
793

794 Jurado, M. J. and Riba, O.: The Rioja area (westernmost Ebro basin): a ramp valley with  
795 neighbouring piggybacks, in: Friend, P. and Dabrio, C. (Eds.): *Tertiary basins of Spain*, *World*  
796 *and Regional Geology*, 6, Cambridge University Press, Cambridge, 173-179, 1996.  
797

798 Kirby, E. and Whipple, K. X.: Expression of active tectonics in erosional landscapes, *J. Struct.*  
799 *Geol.*, 44, 54-75, <https://doi.org/10.1016/j.jsg.2012.07.009>, 2012.  
800

801 Kuhlemann, J., Frisch, W., Dunkl, I., Székely, D., and Spiegel, C.: Miocene shifts of the  
802 drainage divide in the Alps and their foreland basin, *Z. Geomorph.*, 45, 239-265, 2001.  
803

804 Lacan, P. and Ortuño, M.: Active tectonics of the Pyrenees: a review, *J. Iberian Geol.*, 38, 9-30,  
805 [https://doi.org/10.5209/rev\\_JIGE.2012.v38.n1.39203](https://doi.org/10.5209/rev_JIGE.2012.v38.n1.39203), 2012.  
806



807 Larrasoña, J. C., Murelaga, X., and Garcés, M.: Magnetobiochronology of Lower Miocene  
808 (Ramblian) continental sediments from the Tuleda Formation (western Ebro basin, Spain), *Ea.*  
809 *Planet. Sci. Lett.*, 243, 409-423, <https://doi.org/10.1016/j.epsl.2006.01.034>, 2006.  
810

811 López-Blanco, M., Marzo, M., Burbank, D. W., Vergés, J., Roca, E., Anadón, P., and Piña, J.:  
812 Tectonic and climatic controls on the development of foreland fan deltas: Montserrat and Sant  
813 Llorenç del Munt systems (Middle Eocene, Ebro Basin, NE Spain), *Sediment. Geol.*, 138, 17-  
814 39, 2000.  
815

816 López-Martínez, N., García-Moreno, E., and Álvarez-Sierra, A.: Paleontología y  
817 bioestratigrafía (micromamíferos) del Mioceno medio y superior del sector central de la cuenca  
818 del Duero, *Studia Geologica Salmanticensia*, Ediciones Universidad Salamanca, 22, 191-212,  
819 1986.  
820

821 Martín-Chivelet, J., Berástegui, X., Rosales, I., Vilas, L., Vera, J. A., Caus, E., Gräfe, K. U.,  
822 Mas, R., Puig, C., Segura, M., Robles, S., Floquet, M., Quesada, S., Ruiz-Ortiz, P. A., Fregenal-  
823 Martínez, M. A., Salas, R., Arias, C., García, A., Martín-Algarra, A., Meléndez, M. N., Chacón,  
824 B., Molina, J. M., Sanz, J. L., Castro, J. M., García-Hernández, M., Carenas, B., García-  
825 Hidalgo, J., Gil, J., and Ortega, F.: Cretaceous, in: *The Geology of Spain*, Gibbons, W. and  
826 Moreno, T. (Eds.): The Geological Society, London, 255-292, 2002.  
827

828 Martín-Serrano, A.: La definición y el encajamiento de la red fluvial actual sobre el macizo  
829 hesperico en el marco de su geodinamica alpina, *Rev. Soc. Geol. España*, 4, 337-351, 1991.  
830

831 Mikeš, D.: The Upper Cenozoic evolution of the Duero and Ebro fluvial systems (N-Spain):  
832 Part 1. Paleogeography; Part 2. Geomorphology, *Cent. Eur. J. Geosci.*, 2, 320-332,  
833 <https://doi.org/10.2478/v10085-010-0017-4>, 2010.  
834

835 Montgomery, D. R., Balco, G., and Willett, S. D.: Climate, tectonics, and the morphology of  
836 the Andes, *Geology*, 29, 579-582, 2001.  
837

838 Moreno, D., Falguères, C., Pérez-González, A., Duval, M., Voinchet, P., Benito-Calvo, A.,  
839 Ortega, A. I., Bahain, J. J., Sala, R., Carbonell, E., Bermúdez de Castro, J. M., and Arsuaga, J.  
840 L.: ESR chronology of alluvial deposits in the Arlanzon valley (Atapuerca, Spain):

841 Contemporaneity with Atapuerca Gran Dolina site, *Quat. Geochronol.*, 10, 418-423,  
842 <https://doi.org/10.1016/j.quageo.2012.04.018>, 2012.

843

844 Moreno, D., Belmonte, A., Bartolomé, M., Sancho, C., Oliva, C., Stoll, H., Edwards, L. R.,  
845 Cheng, H., and Hellstrom, J.: Formacion de espeleotemas en el noreste peninsular y su relacion  
846 con las condiciones climaticas durante los ultimos ciclos glaciares, *Cuadernos de Investigacion*  
847 *Geografica*, 39, 25-47, 2013.

848

849 Mudd, S., Attal, M., Milodowski, D. T., Grieve, S. W. D., and Valters, D. A.: A statistical  
850 framework to quantify spatial variation in channel gradients using the integral method of  
851 channel profile analysis, *J. Geophys. Res.- Earth Surf.*, 119, 138-152,  
852 <https://doi.org/10.1002/2013JF002981>, 2014.

853

854 Muñoz-Jiménez, A. and Casas-Sainz, A. M.: The Rioja Trough (N Spain): tectonosedimentary  
855 evolution of a symmetric foreland basin, *Basin Res.*, 9, 65-85, 1997.

856

857 Nivière, B., Lacan, P., Regard, V., Delmas, M., Calvet, M., Huyghe, D., and Roddaz, B.:  
858 Evolution of the Late Pleistocene Aspe River (Western Pyrenees, France). Signature of climatic  
859 events and active tectonics, *Comptes Rendus Geosci.*, 348, 203-212, <https://doi.org/10.1016/j.crte.2015.07.003>, 2016.

860

861

862 Ortigosa, L. M.: Las grandes unidades des relieve, *Geografia de la Rioja*, 1, 62-71, 1994.

863

864 Palacios, D., De Marcos, J., and Vásquez-Selem, L.: Last Glacial Maximum and deglaciation  
865 of the Sierra de Gredos, central Iberian Peninsula, *Quat. Int.*, 233, 16-26,  
866 <https://doi.org/10.1016/j.quaint.2010.04.029>, 2011.

867

868 Palacios, D., Andrés, N., De Marcos, J., and Vásquez-Selem, L.: Maximum glacial advance and  
869 deglaciation of the Pinar Valley (Sierra de Gredos, Central Spain) and its significance in the  
870 Mediterranean context, *Geomorph.*, 177-178, 51-61,  
871 <https://doi.org/10.1016/j.geomorph.2012.07.013>, 2012.

872

873 Pellicer, F. and Echeverría, M. T.: El modelado glaciar y periglaciar en el macizo del moncayo,  
874 in: Peña, J. L., Longares, L. A., and Sánchez, M. (Eds.): *Geografía Física de Aragon*, Aspetos

875 generals y tematicos, Universidad de Zaragoza e Institucion Fernado el Catolico, Zaragoza,  
876 173-185, 2004.

877

878 Pérez-Rivarés, F. J., Garcés, M., Arenas, C., and Pardo, G.: Magnetocronologia de la sucesion  
879 Miocena de la Sierra de Alcubierre (sector central de la cuenca del Ebro), *Rev. Soc. Geol.*  
880 *España*, 15, 217-231, 2002.

881

882 Pérez-Rivarés, F. J., Garcés, M., Arenas, C., and Pardo, G.: Magnetostratigraphy of the Miocene  
883 continental deposits of the Montes de Castejon (central Ebro basin, Spain): geochronological  
884 and paleoenvironmental implications, *Geologica Acta*, 2, 221-234, 2004.

885

886 Perron, J. T. and Royden, L.: An integral approach to bedrock river profile analysis. *Earth Surf.*  
887 *Process. Landforms*, 38, 570–576, <https://doi.org/10.1002/esp.3302>, 2012.

888

889 Pineda Velasco, A.: Montorio. Mapa geologico de España; escala 1:50.000; Segunda serie.  
890 Instituto Geologico y Minero de España (IGME), Madrid, pp. 110, 1997.

891

892 Prince, P. S., Spotila, J. A., and Henika, W. S.: Stream capture as driver of transient landscape  
893 evolution in a tectonically quiescent setting, *Geology*, 39, 823–826,  
894 <https://doi.org/10.1130/G32008.1>, 2011.

895

896 Puigdefàbregas, C., Muñoz, J. A., and Vergés, J.: Thrusting and foreland basin evolution in the  
897 Southern Pyrenees, in: *Thrust Tectonics*, McClay, K.R. (Ed.): Chapman & Hall, London, 247-  
898 254, 1992.

899

900 Pulgar, J. A., Alonso, J. L., Espina, R. G., and Marín, J. A.: La deformacion alpine en el  
901 basamento varisco de la Zona Cantabrica, 283-294, 1999.

902

903 Riba, O., Reguant, S., and Villena, J.: Ensayo de sintesis estratigrafica y evolutiva de la Cuenca  
904 terciaria del Ebro, in: Comba, J. A. (Ed.): *Geologia de España*, 2, Libro Jubila J. M. Rios,  
905 Instituto Geologico y Minero de España, Madrid, 131-159, 1983.

906

907 Rivas-Carballo, M. R., Alonso-Gavilán, G., Valle, M. F., and Civis, J.: Miocene Palynology of  
908 the central sector of the Duero Basin (Spain) in relation to palaeogeography and  
909 palaeoenvironment, *Rev. Palaeobot. Palynol.*, 82, 251-264, 1994.

910

911 Salas, R., Guimerà, J., Mas, R., Martín-Closas, C., Meléndez, A., and Alonso, A.: Evolution of  
912 the Mesozoic Central Iberian Rift System and its Cainozoic inversion (Iberian Chain), in:  
913 Ziegler, P. A., Cavazza, W., Robertson, A. F. H., and Crasquin-Soleau, S. (Eds.): *Peri-Tethys*  
914 *Memoir 6: Peri-Tethyan Rift/Wrench Basins and Passive Margins. Mémoires du Muséum*  
915 *national d'Histoire naturelle*, 186, 145-185, 2001.

916

917 Sancho, C., Calle, M., Peña-Monné, J. L., Duval, M., Oliva-Urcia, B., Pueyo, E. L., Benito, G.,  
918 and Moreno, A.: Dating the Earliest Pleistocene alluvial terrace of the Alcanadre River (Ebro  
919 Basin, NE Spain): Insights into the landscape evolution and involved processes, *Quat. Int.*, 407,  
920 86-95, <https://doi.org/10.1016/j.quaint.2015.10.050>, 2016.

921

922 Schumm, S. A., Mosley, M. P., and Weaver, W. E.: *Experimental fluvial geomorphology*, John  
923 Wiley and Sons, New York, pp. 413, 1987.

924

925 Schwanghart, W. and Scherler, D.: TopoToolbox 2 a MATLAB-based software for topographic  
926 analysis and modeling in Earth surface sciences, *Earth Surf. Dynamics*, 2, 1-7,  
927 <https://doi.org/10.5194/esurf-2-1-2014>, 2014.

928

929 Serrano, E., González-Trueba, J. J., Pellitero, R., González-García, M., and Gómez-Lende, M.:  
930 Quaternary glacial evolution in the Central Cantabrian Mountains (Northern Spain),  
931 *Geomorph.*, 196, 65-82, <https://doi.org/10.1016/j.geomorph.2012.05.001>, 2013.

932

933 Serrano, E., González-Trueba, J. J., Pellitero, R., Gómez-Lende, M.: Quaternary glacial history  
934 of the Cantabrian Mountains of northern Spain: a new synthesis, in: Hughes, P. D. and  
935 Woodward, J. C. (Eds.): *Quaternary Glaciation in the Mediterranean Mountains*, Geological  
936 Society, London, Special Publications, 433, <https://doi.org/10.1144/SP433.8>, 2016.

937

938 Sobel, E. R. and Strecker, M. R.: Uplift, exhumation and precipitation: tectonic and climatic  
939 control of Late Cenozoic landscape evolution in the northern Sierras Pampeanas, Argentina,  
940 *Basin Res.*, 15, 431-451, <https://doi.org/10.1046/j.1365-2117.2003.00214.x>, 2003.

941

942 Sobel, E. R., Hilley, G. E., and Strecker, M. R.: Formation of internally drained contractional  
943 basins by aridity-limited bedrock incision, *J. Geophys. Res.*, 108, 2344,  
944 <https://doi.org/10.1029/2002JB001883>, 2003.

945

946 Stange, K. M., Van Balen, R. T., Garcia-Castellanos, D., and Cloething, S.: Numerical  
947 modelling of Quaternary terrace staircase formation in the Ebro foreland basin, southern  
948 Pyrenees, NE Iberia, *Basin Res.*, 1-23, <https://doi.org/10.1111/bre.12103>, 2014.

949

950 Suc, J. P. and Popescu, S. M.: Pollen records and climatic cycles in the Mediterranean region  
951 since 2.7 Ma, in: Head, M. J. and Gibbard, P. L. (Eds.): *Early-Middle Pleistocene Transitions,*  
952 *the Land-Ocean Evidence*, Geological Society, London, Special Publications, 247, 147-158,  
953 <https://doi.org/10.1144/GSL.SP.2005.247.01.08>, 2005.

954

955 Urgeles, R., Camerlenghi, A., Garcia-Castellanos, D., De Mol, B., Garcés, M., Vergés, J.,  
956 Haslam, I., and Hardman, M.: New constraints on the Messinian sealevel drawdown from 3D  
957 seismic data of the Ebro Margin, western Mediterranean, *Basin Res.*, 23, 123-145,  
958 <https://doi.org/10.1111/j.1365-2117.2010.00477.x>, 2010.

959

960 Van der Beek, P., Litty, C., Baudin, M., Mercier, J., Robert, X., and Hardwick, E.: Contrasting  
961 tectonically driven exhumation and incision patterns, Western versus central Nepal Himalaya,  
962 *Geology*, 44, 327-330, <https://doi.org/10.1130/G37579.1>, 2016.

963

964 Vázquez-Urbez, M., Arenas, C., Pardo, G., and Pérez-Rivarés, J.: The effect of drainage  
965 reorganization and climate on the sedimentologic evolution of intermontane lake systems: the  
966 final fill stage of the Tertiary Ebro Basin (Spain), *J. Sediment. Res.*, 83, 562-590,  
967 <https://doi.org/10.2110/jsr.2013.47>, 2013.

968

969 Villena, J., Pardo, G., Pérez, A., Muñoz, A., and González, A.: The Tertiary of the Iberian margin  
970 of the Ebro basin: palaeogeography and tectonic control, in: Friend, P. and Dabrio, C. (Eds.):  
971 *Tertiary basins of Spain, World and Regional Geology*, 6, Cambridge University Press,  
972 Cambridge, 83-88, 1996.

973

974 Whipple, K.: The influence of climate on the tectonic evolution of mountain belts, *Nature*  
975 *Geosci.*, 2, 97-104, <https://doi.org/10.1038/ngeo638>, 2009.

976

977 Whipple, K. X. and Tucker, G. E.: Dynamics of the stream-power river incision model:  
978 Implications for height limits of mountain ranges, landscape response timescales, and research  
979 needs, *J. Geophys. Res.*, 104, 17661-17674, 1999.

980

981 Whipple, K. X., Forte, A. M., DiBiase, R. A., Gasparini, N. M., Ouimet, W. B.: Timescales of  
982 landscape response to divide migration and drainage capture: implications for the role of divide  
983 mobility in landscape evolution, *J. Geophys. Res.- Ea. Surf.*, 122, 248-273,  
984 <https://doi.org/10.1002/2016JF003973>, 2017.

985

986 Whitfield, E. and Harvey, A. M.: Interaction between the controls on fluvial system  
987 development: tectonics, climate, base level and river capture – Rio Alias, Southeast Spain, *Earth*  
988 *Surf. Process. Landforms*, 37, 1387-1397, <https://doi.org/10.1002/esp.3247>, 2012.

989

990 Willett, S. D.: Orogeny and orography: The effects of erosion on the structure of mountain belts,  
991 *J. Geophys. Res.*, 104, 28957-28981, 1999.

992

993 Willett, S. D., McCoy, S. W., Perron, J. T., Goren, L., and Chen, C. Y.: Dynamic reorganization  
994 of river basins, *Science*, 343, 1248765, <https://doi.org/10.1126/science.1248765>, 2014.

995

996 Yanites, B. J., Elhers, T. A., Becker, J. K., Schnellmann, M., and Heuberger, S.: High magnitude  
997 and rapid incision from river capture: Rhine River, Switzerland, *J. Geophys. Res.- Ea. Surf.*,  
998 118, 1060-1084, <https://doi.org/10.1002/jgrf.20056>, 2013.

999

1000

1001

1002

1003

1004

1005

1006

1007

Figure captions:

Figure 1: A) Topographic map of the Duero and Ebro basins and surrounding belts. B) Averaged topographic section throughout the Duero and Ebro basins showing important incision contrast between the two basins. The Duero basin recorded low incision, especially in its upper part, whereas the Ebro basin is highly excavated.

Figure 2: Simplified geological map of the study area.

Figure 3: Topographic map of the study area with all the rivers considered in this study. The red lines represent drainage divides between main hydrographic basins.

Figure 4: Zoom in the geological map of the Iberian Range showing the location of the Jalon river tributaries. The river long profiles of these streams and the location of knickpoints are shown to the left.

Figure 5: A) Zoom in the geological map of the Bureba sector. B) Zoom in the Homino river (Ebro tributary) capturing the upper reach of the Jordan river (Duero tributary). C) Schematic representation of this capture using river long profiles and map orientation, showing the associated knickpoint and wind gap.

Figure 6: Mean annual precipitation map for the study area (data from Hijmans et al., 2005).

Figure 7: A) 3D view of the DEM of the Bureba sector showing important contrast of incision between the Ebro and Duero basins across their divide (red dashed line) and river capture evidence (elbows of capture, knickpoints and wind gaps). B) Google Earth image around the locality of Hontomin where the Homino river is capturing the upper reach of the Jordan river. C) and D) Wind gaps cut into the Bureba anticline (see location on Fig. 7A). Pictures have been taken from the north of this structure toward the south. E) Possible three steps evolution of the southwestward divide retreat through multiple river captures witnessed in the area.

Figure 8: River long profiles for all the streams described in the Bureba area showing evidence of river capture. Colors are given to rivers that are linked in these capture processes.

Figure 9: Topographic map showing the location of all the knickpoints and low relief surfaces that may be associated to river capture. The black dashed line represents a possible paleodrainage divide between the Ebro and Duero basins. The area between this dashed line and the present-day location of the divide in red may have belonged the Duero basin before being captured by the Ebro basin.

Figure 10: Duero river long profile (black line) and difference in the specific stream power of the river (grey) calculated by considering the paleo and present-day position of its divide. Positive values suggest a significant diminution of the incision capacity of the Duero river, particularly along the knickzone of its longitudinal profile. Details on calculation are available in the Supplement (Section S1).

Figure 11: Topographic map with  $\chi$  values calculated on different opposite streams in the vicinity of the Ebro/Duero drainage divide. This map shows significant contrasting values between the Ebro and Duero drainage networks.



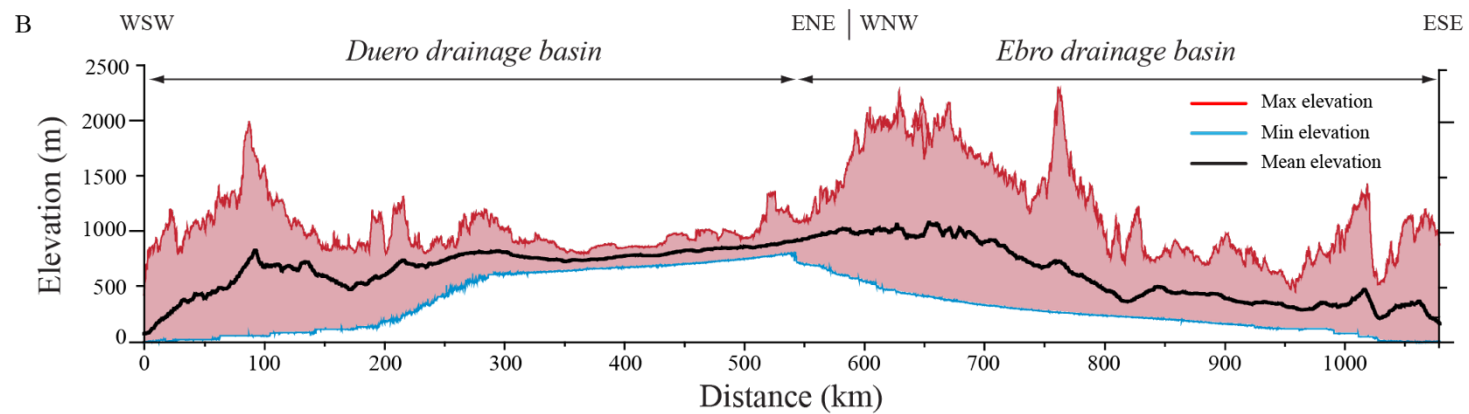
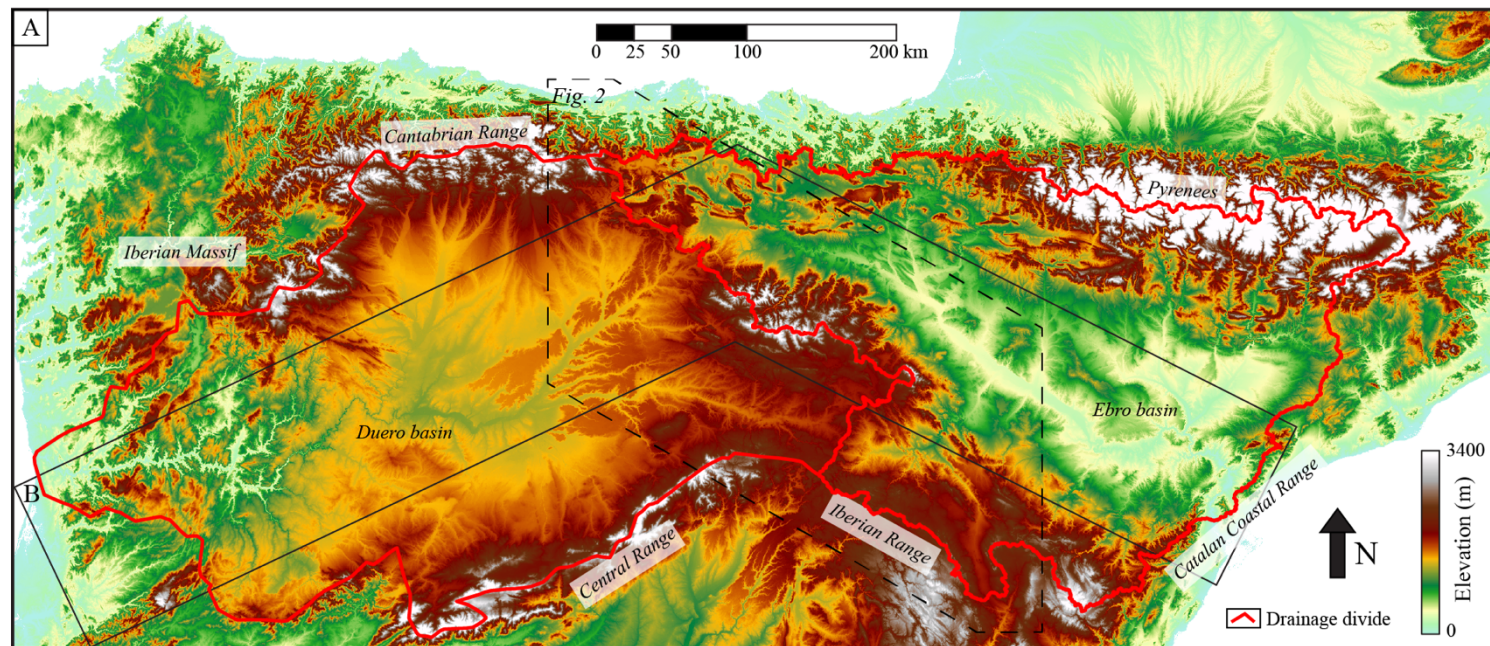


Figure 1

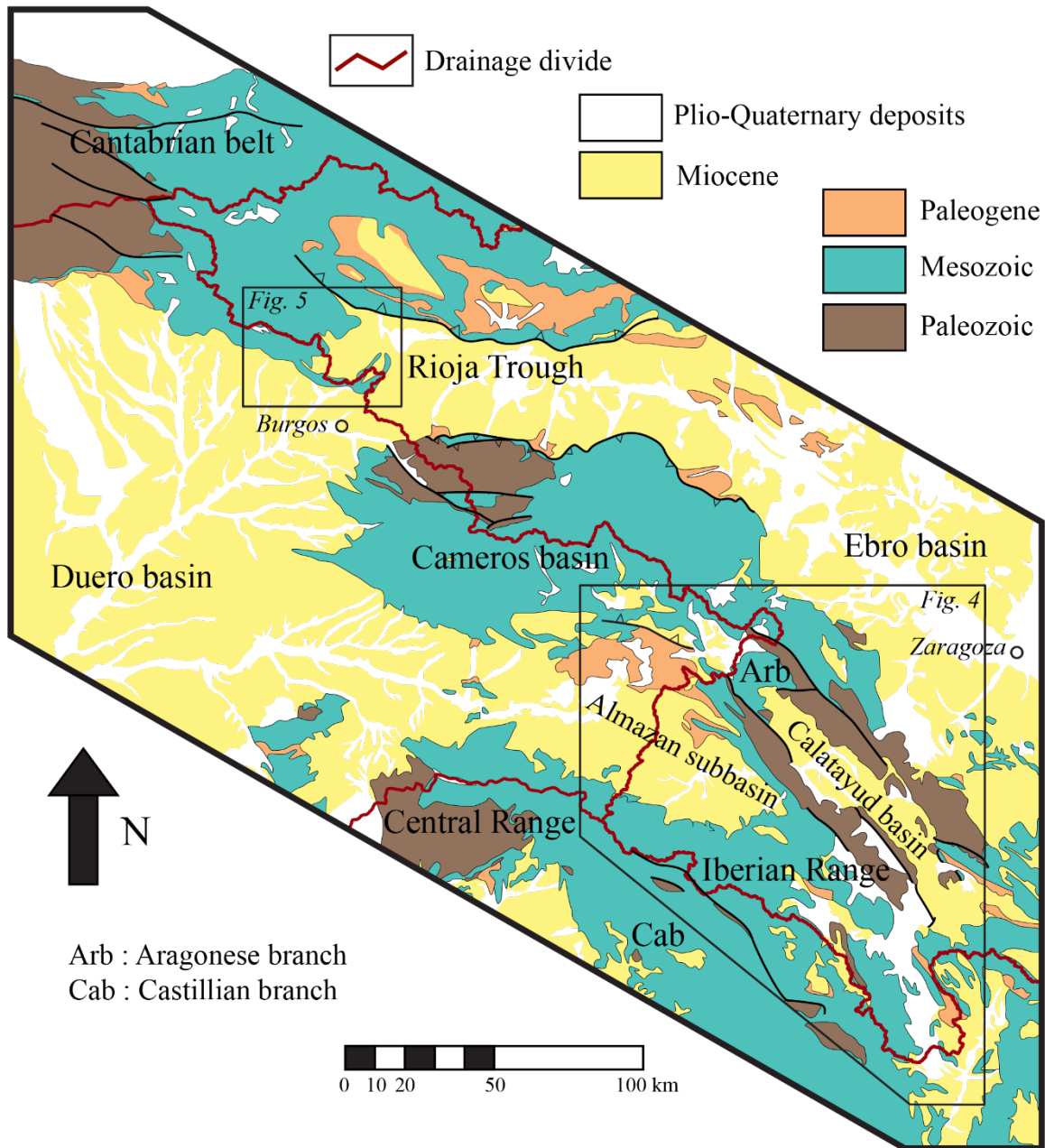


Figure 2

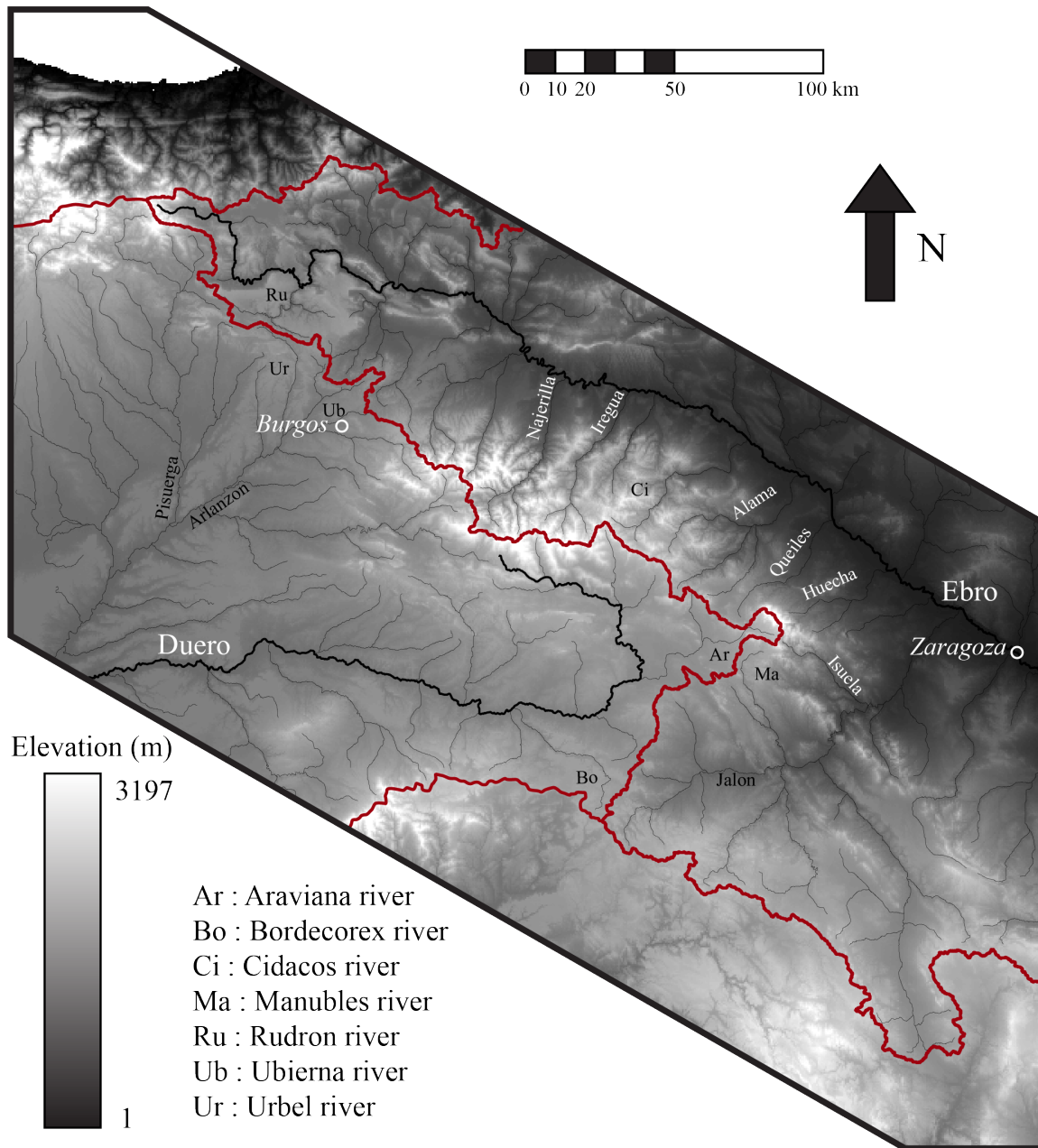


Figure 3

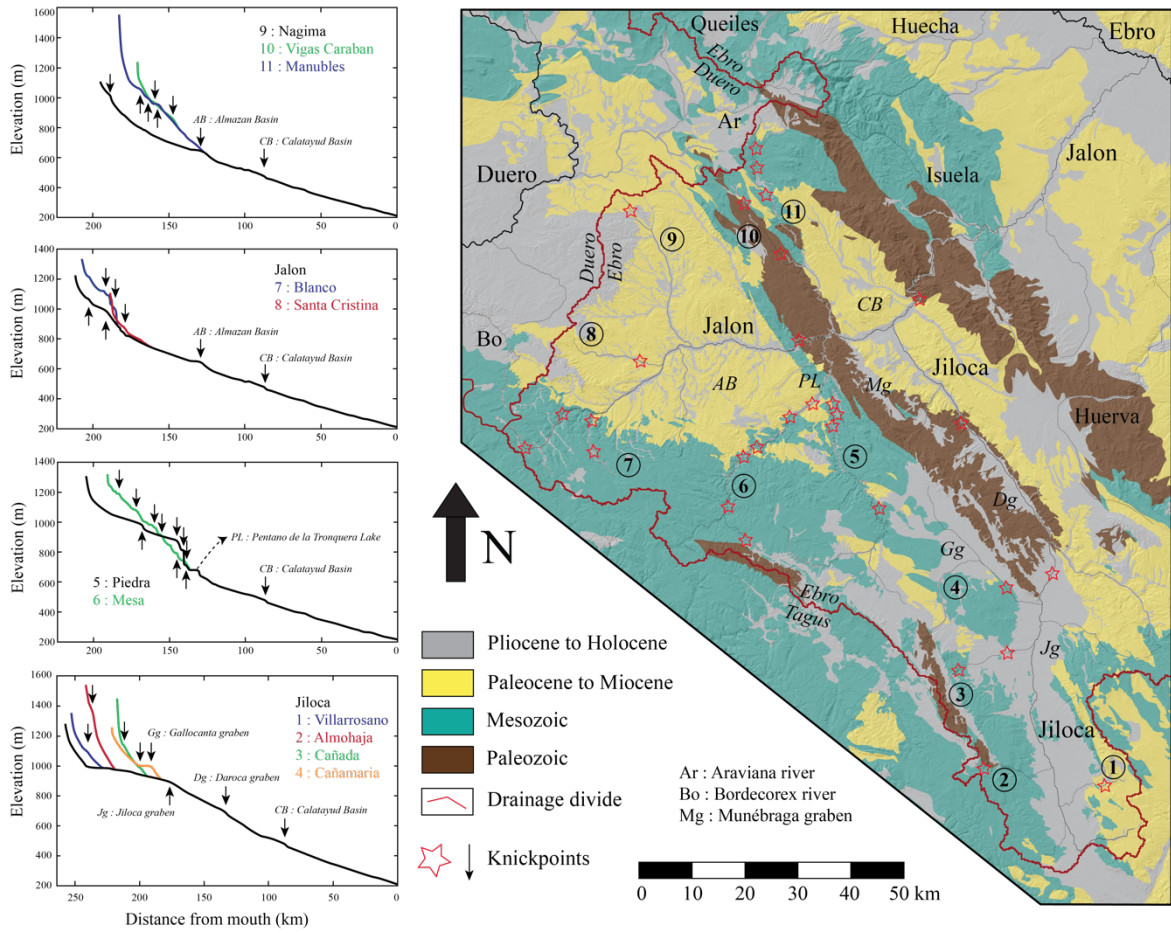


Figure 4

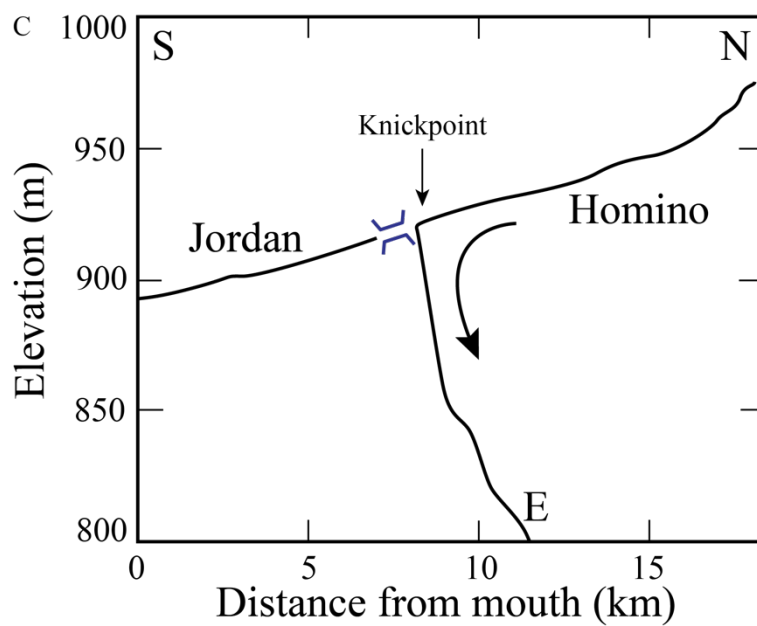
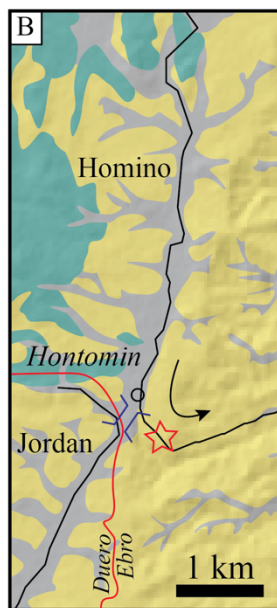
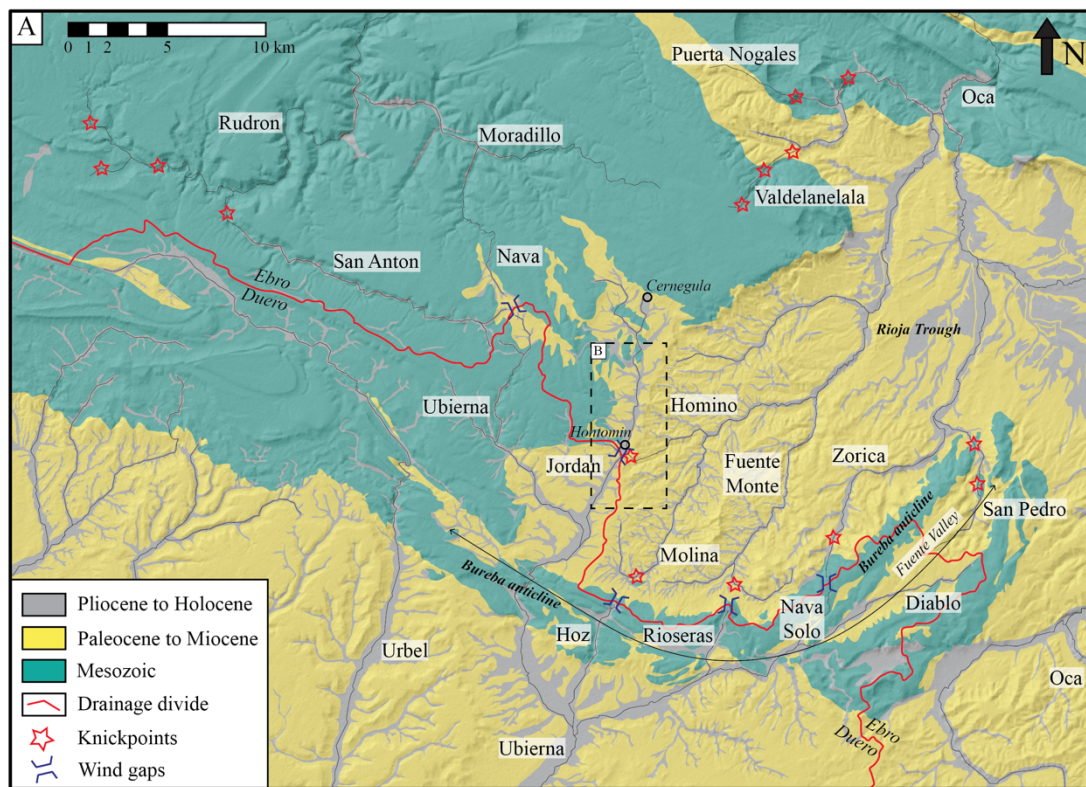


Figure 5

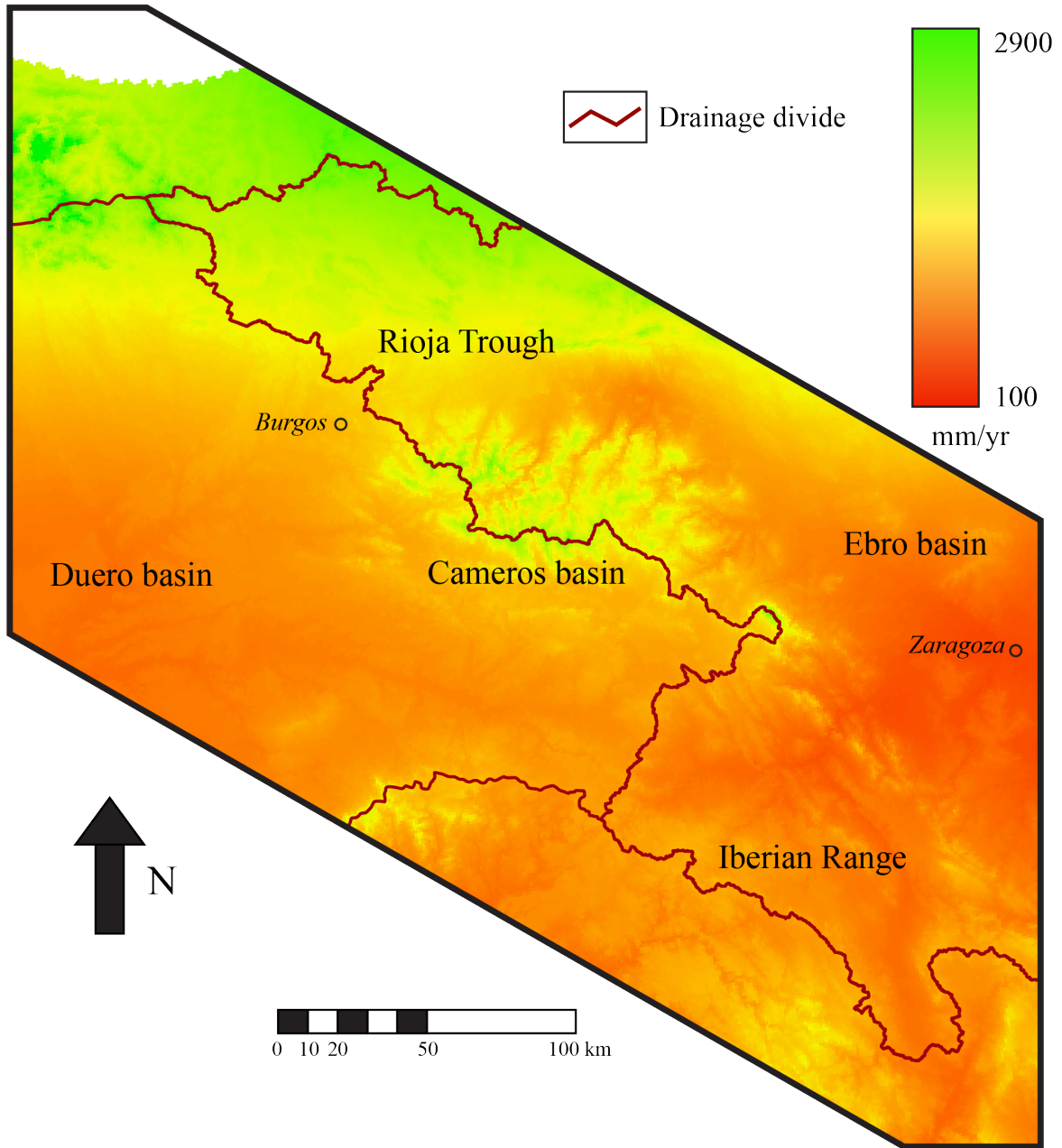
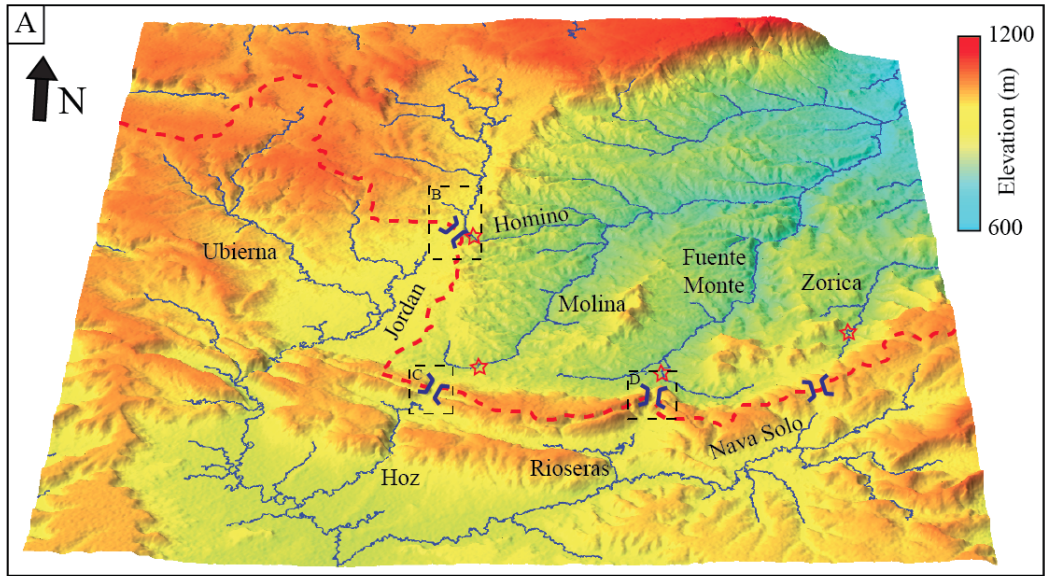


Figure 6



- Drainage divide
- Knickpoints
- Wind gaps
- Mesozoic relief
- Cenozoic incision

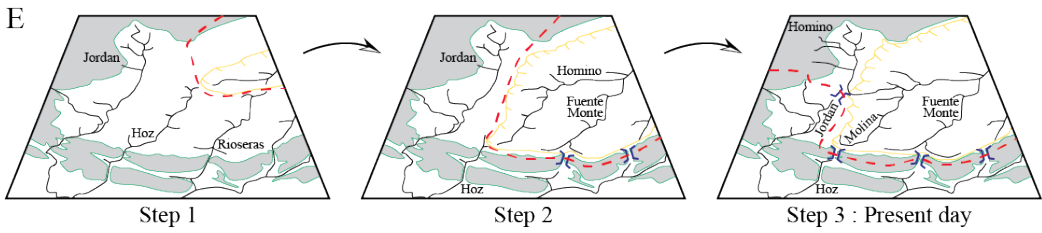
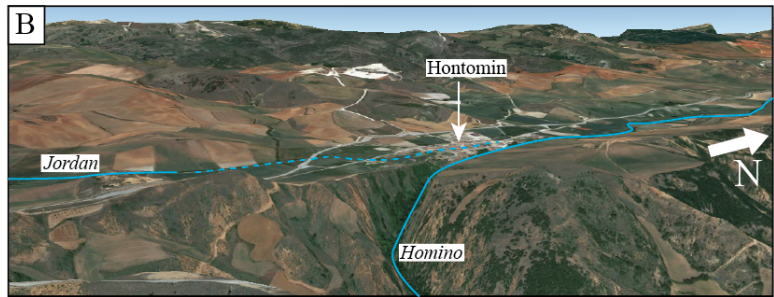


Figure 7

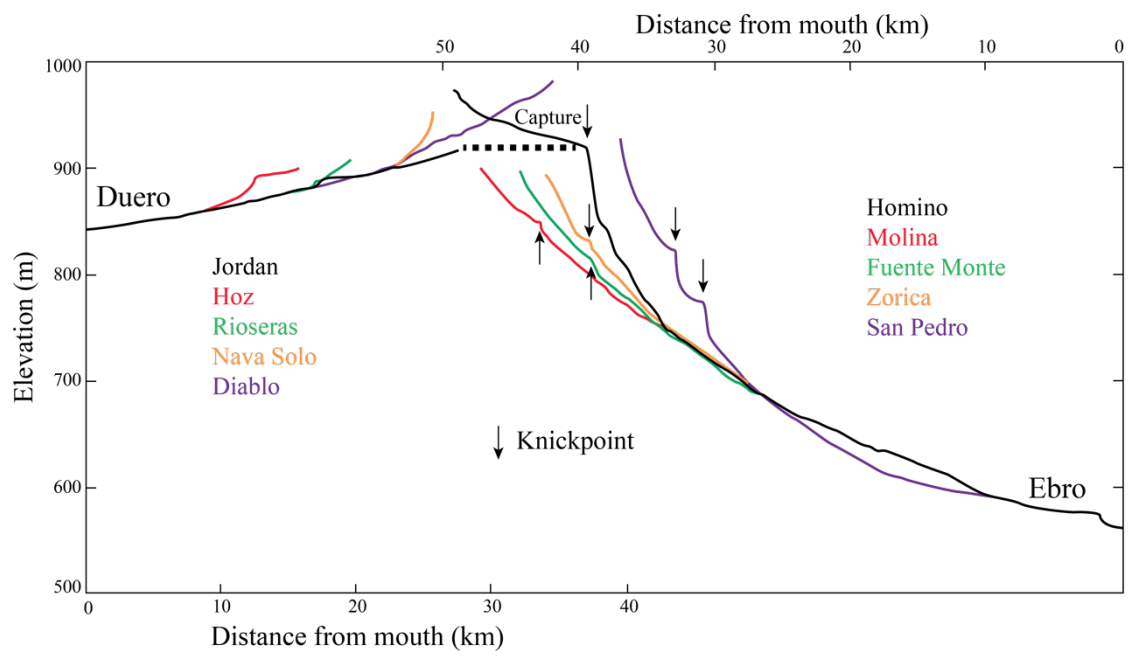


Figure 8



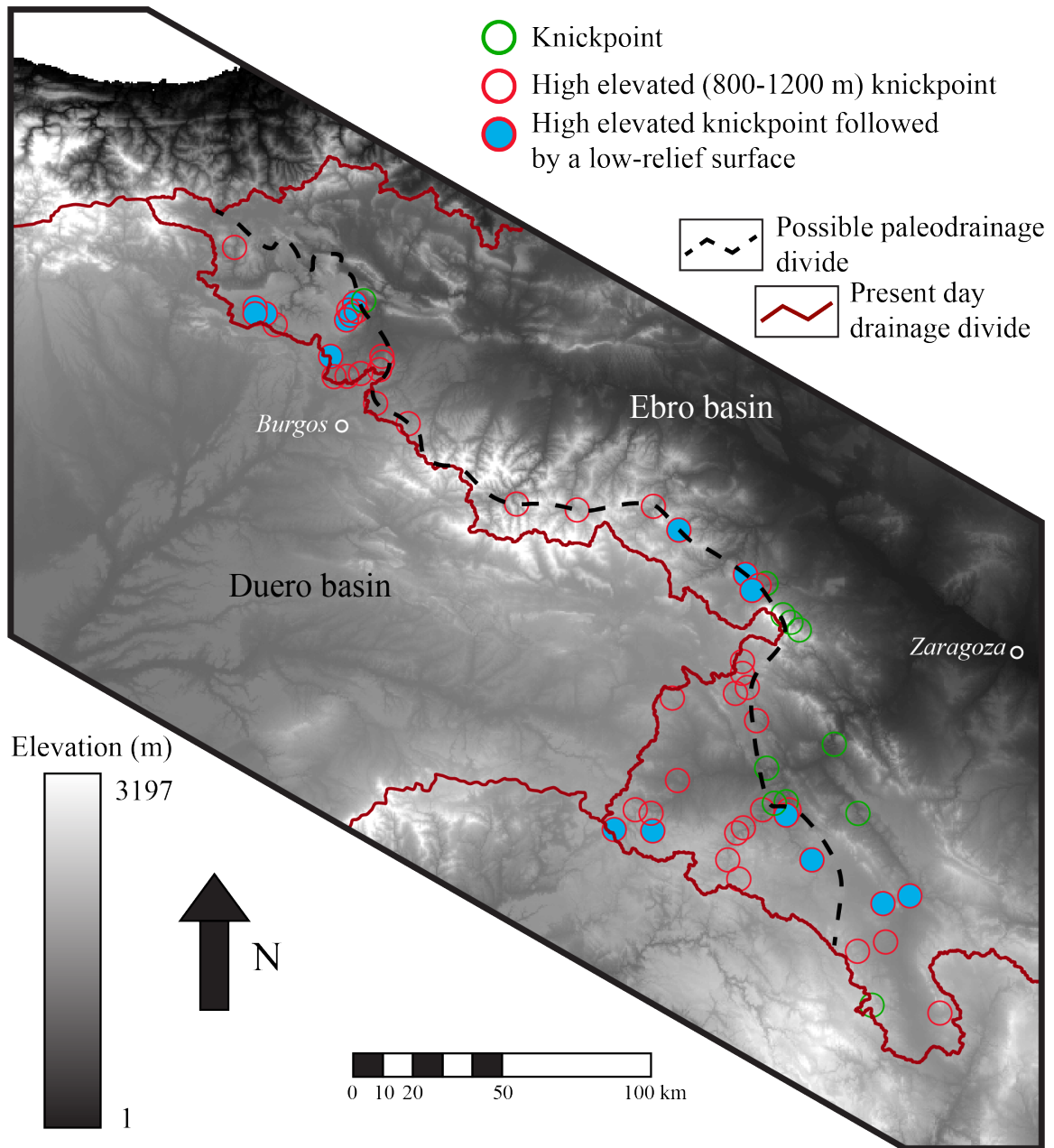


Figure 9

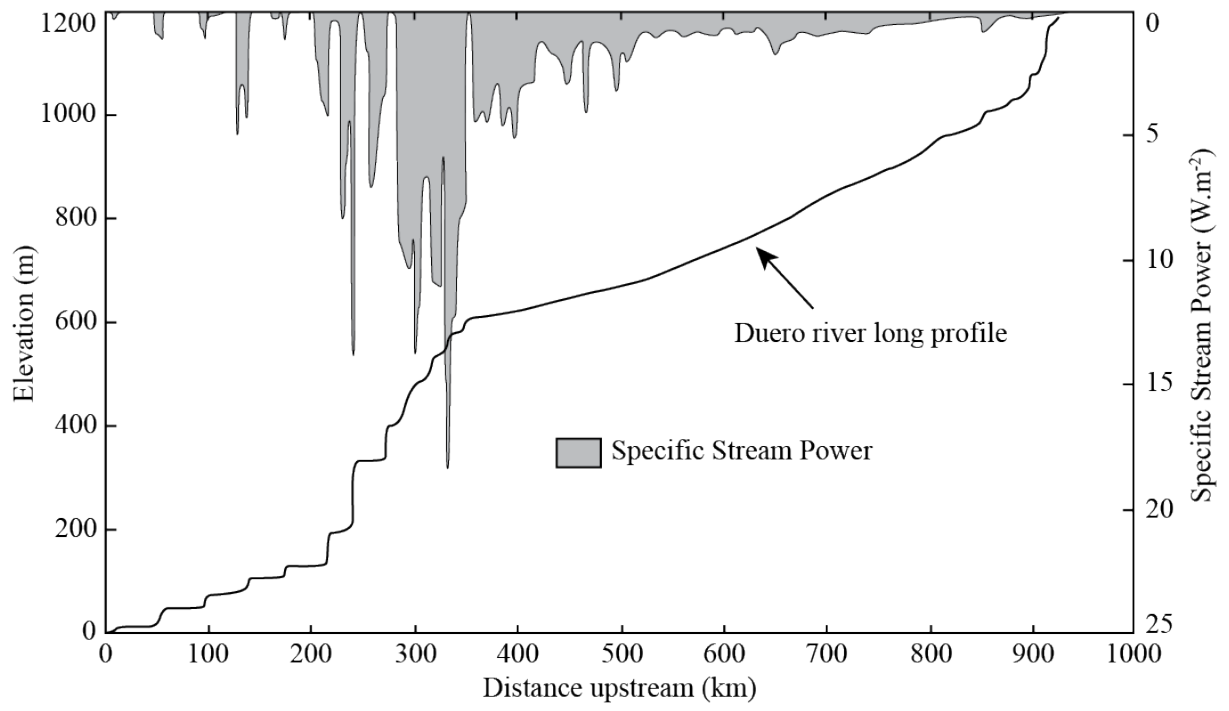


Figure 10

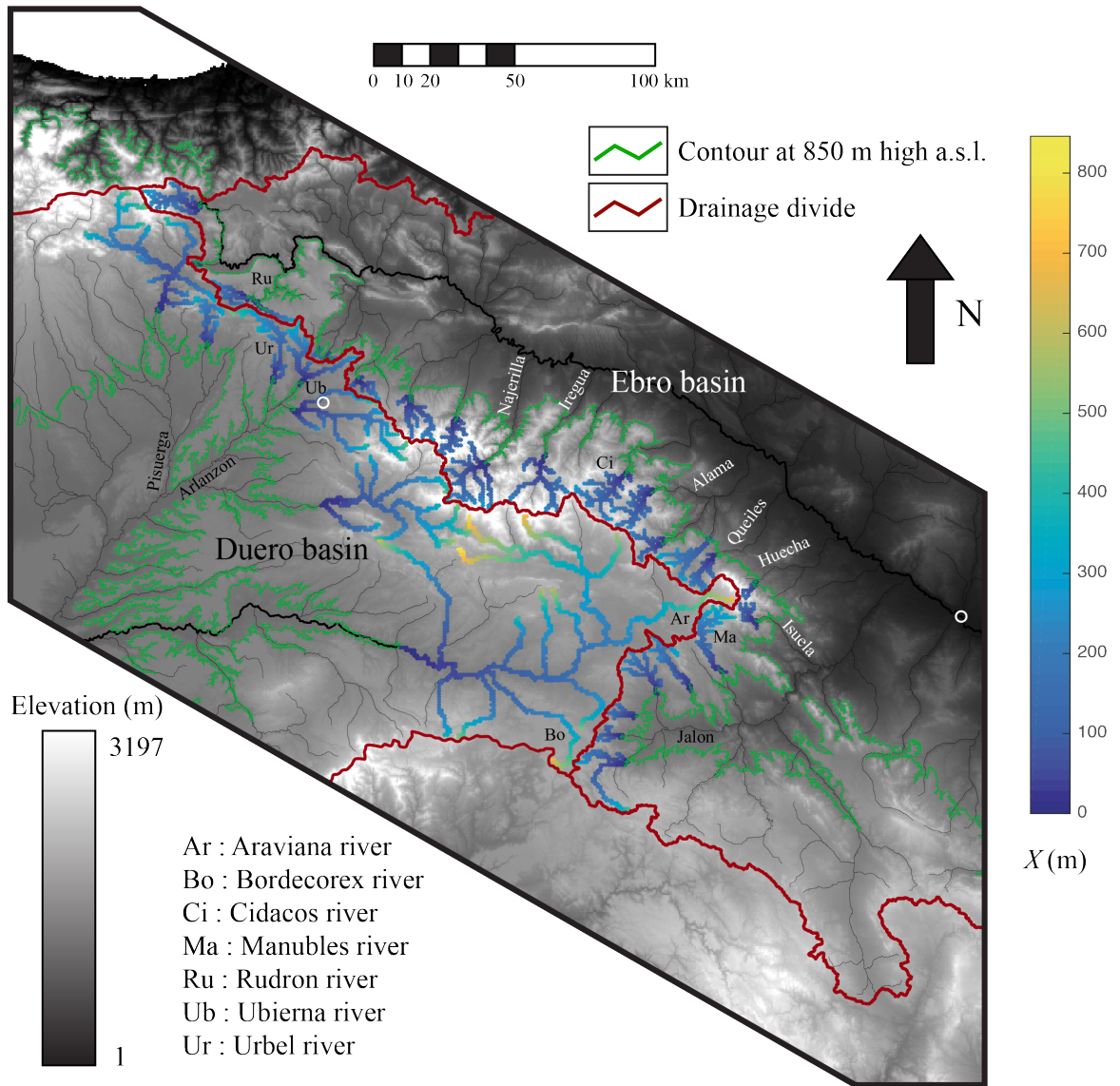


Figure 11